White paper

Lung Ultrasound in Patients with Coronavirus COVID-19 Disease

Dirk-André Clevert, MD
Professor of Radiology
Section Chief of the Interdisciplinary Ultrasound Center
at the Department of Clinical Radiology
University of Munich Hospitals, Grosshadern Campus

siemens-healthineers.com/ultrasound

SIEMENS Healthineers

Lung Ultrasound in Patients with Coronavirus COVID-19 Disease

Dirk-André Clevert, MD
Professor of Radiology
Section Chief of the Interdisciplinary Ultrasound Center
at the Department of Clinical Radiology
University of Munich Hospitals, Grosshadern Campus

Contents

Introduction	3
Basics of lung ultrasound	5
Artifacts	7
Transducer selection and settings	11
Image fusion	13
Examination procedure	14
Basic lung exam	15
Summary of Coronavirus COVID-19 examination and follow-up	21
References	24

Introduction

According to the Center for Systems Science and Engineering (CSSE) at Johns Hopkins University (JHU), Coronavirus COVID-19 disease increased daily worldwide. On March 20, 2020 at 8 a.m. European time, there were 81,199 officially reported confirmed COVID-19 cases in China, 163,324 cases in the rest of the world. The number of Coronavirus cases increased rapidly in the United States of America and Europe [1].

The World Health Organization (WHO) announced a pandemic infection with an unknown species of coronavirus called SARS-CoV-2 [2].

According to Wujtewicz, spreading mainly through the droplet route, the virus causes mild symptoms in the majority of cases, the most common being: fever (80%), dry cough (56%), fatigue (22%) and muscle pain (7%); less common symptoms include a sore throat, a runny nose, diarrhea, hemoptysis and chills [3]. A life-threatening complication of SARS-CoV-2 infection is an acute respiratory distress syndrome (ARDS), which occurs more often in older adults, those with immune disorders and co-morbidities. Severe forms of the infection, being an indication for treatment in the intensive care unit (ICU), comprise of acute lung inflammation, ARDS, sepsis and septic shock [3].

Critically ill patients frequently need thoracic imaging due to the constant evolution of their clinical conditions [4]. A key part of monitoring critical patients in the ICU is thoracic ultrasound, as it allows the intensivist to examine the lung and pleural space [5–6]. High-resolution computed tomography (HR-CT) scans remains the gold standard imaging technique for thoracic evaluation, but transportation of patients outside the ICU is difficult and potentially harmful [7]. HR-CT scans expose patients to doses of radiation and should be reserved for specific situations (e.g., the evaluation of mediastinal pathologies and confirmation of pulmonary embolism) [8–10]. Bedside chest X-ray (CXR) is still considered the standard of care for many diagnostic applications in the ICU. However, this imaging technique has important methodological limitations and often yields low accuracy [11]. Furthermore, it is important to consider radioprotection issues. As lung abnormalities may develop before clinical manifestations and nucleic acid detection, experts have recommended early chest CT for screening suspected patients [12]. The high contagiousness of SARS-CoV-2 and the risk of transporting unstable patients with hypoxemia and hemodynamic failure, make chest CT a limited option for the patient with suspected or established COVID-19 [12]. Lung ultrasonography (LUS) gives results that are similar to HR-CT and superior to standard chest CXR for evaluation of pneumonia and/or ARDS with the added advantage of ease of use at point of care, repeatability, absence of radiation exposure, and low cost [12–13]. Cumulative ionizing radiation has known harmful effects. [14] The use of bedside ultrasound could reduce standard CXR and HR-CT in the ICU [5–6].

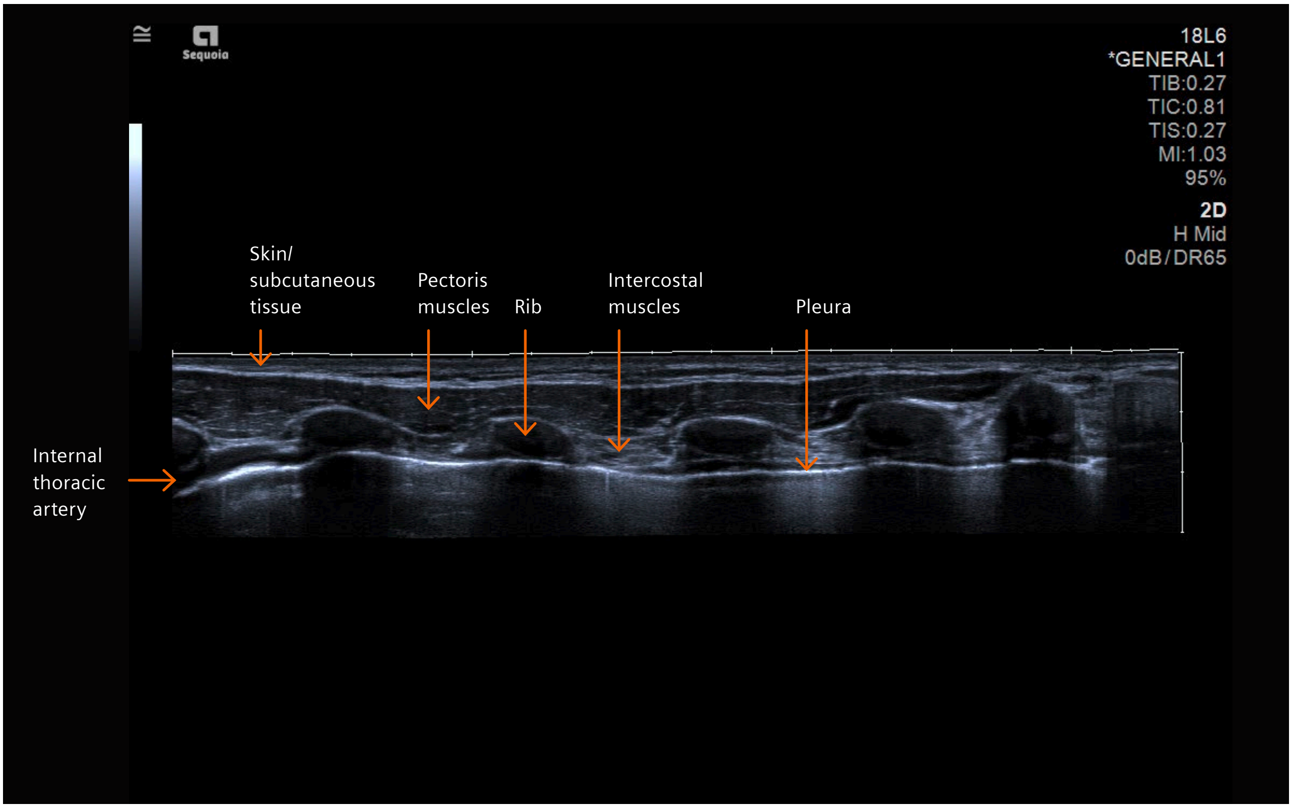

Figure 1: Anatomical basics of the superficial chest wall structures and lung using the panoramic view.

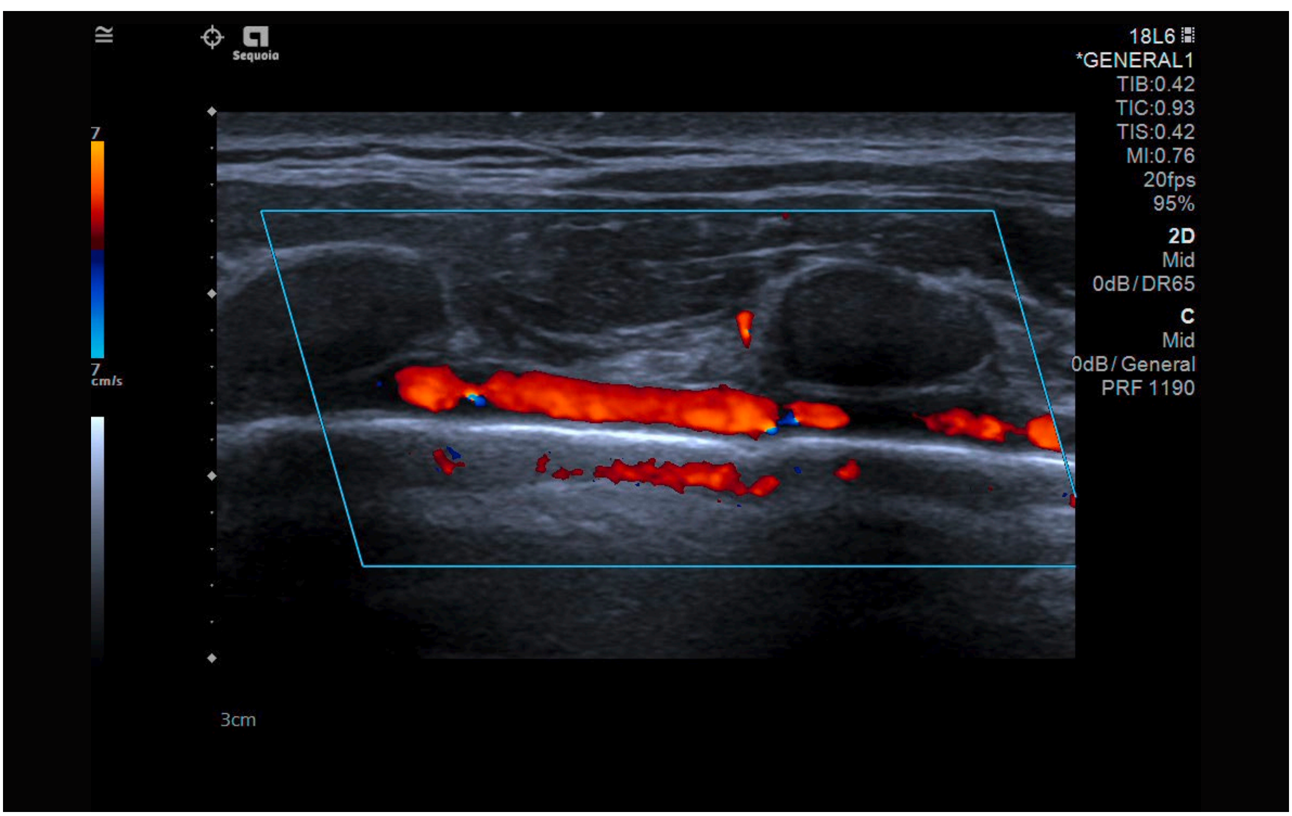

Figure 2: Anatomical basics of the chest wall structures and the internal thoracic artery using the color Doppler examination.

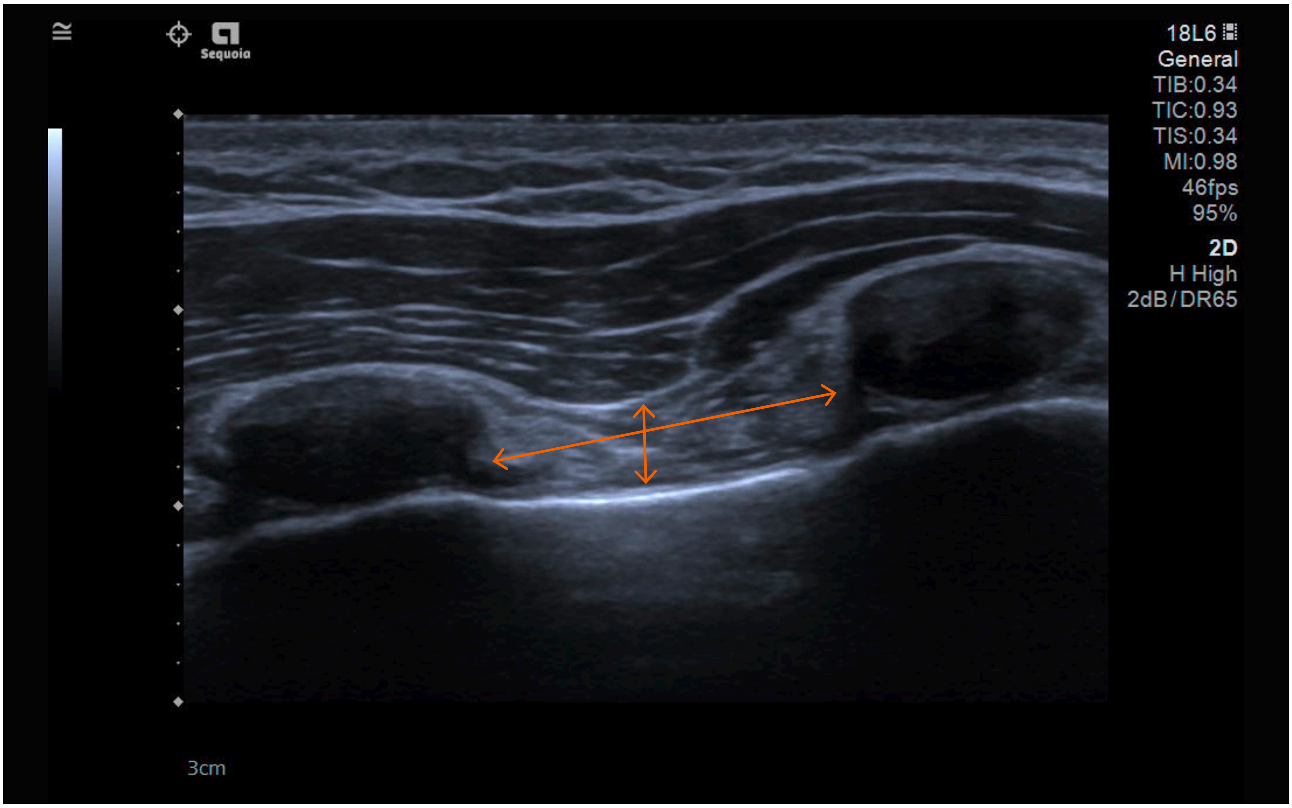

Figure 3: Dynamic examination of the intercostal muscles. Relaxation of the muscle during expiration.

Basics of lung ultrasound examinations

Thorax and lung sonography (LUS) have gained importance in daily routine [15–20] which is especially true in the setting of point-of-care ultrasound (POCUS) [21] **(Figure 1)**.

The first sonographic examinations of the lung were performed more than 50 years ago [22–23]. Except for echocardiography used in cardiology and sonography used in obstetrics, ultrasound, in general, was a tool for radiologists, and the lung was not considered suitable for this imaging technology [24–26]. Since 1991, intensivists have been using whole-body ultrasound to search for free fluid, vascular access and lung ultrasound [27] **(Figure 2)**.

Acute dyspnoea is a common leading symptom in the ER and ICU. The range of possible differential diagnoses is wide, so after the patient history and physical and vital signs are taken, an urgent portable ultrasound should be performed. Focused lung sonography (LUS) plays a dominant role in emergency sonography alongside focused sonography of the abdomen, heart and lung **(Figures 3–4)**.

Although recommendations exist for elective chest sonography [28–29] and emergency lung sonography [15], point of care lung sonography has not yet been widely used in daily practice [30]. Compared to clinical examination and chest X-ray (CXR), lung sonography

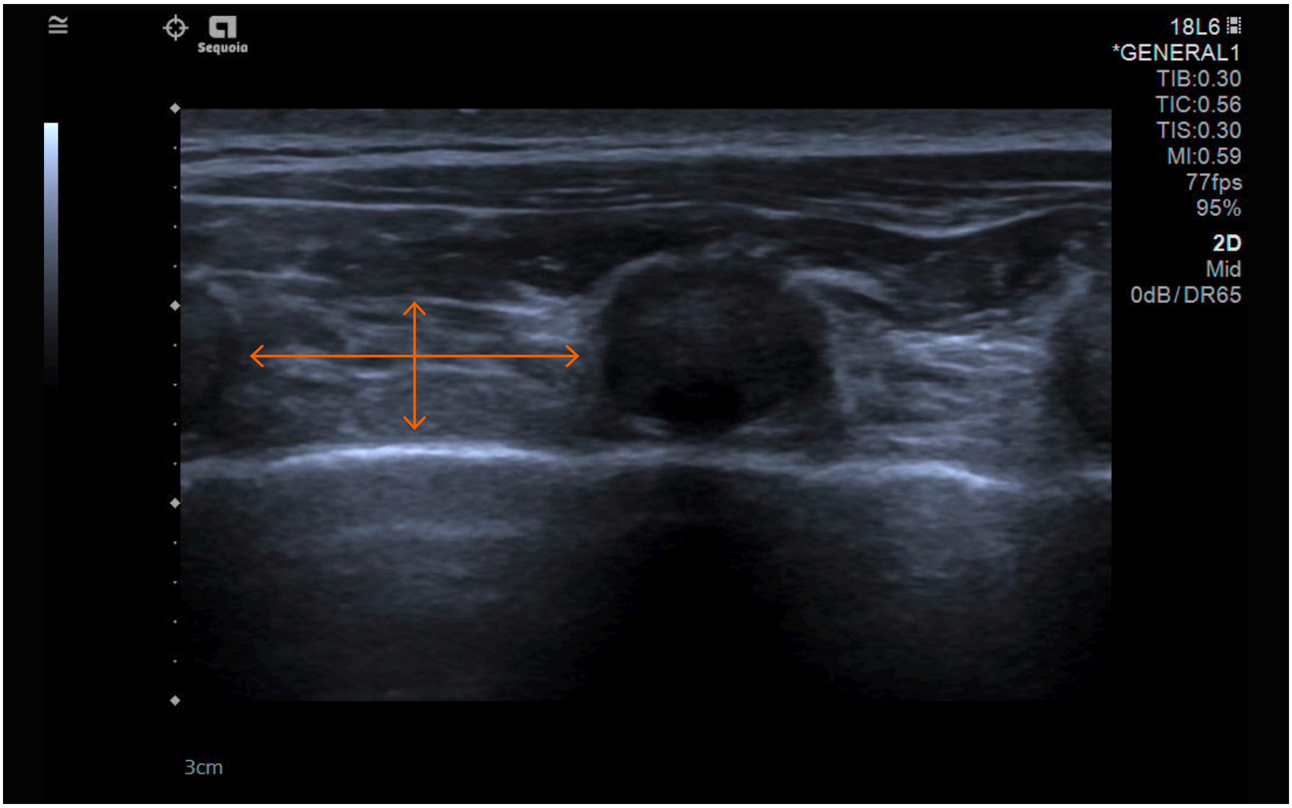

Figure 4: Dynamic examination of the intercostal muscles. Contraction of the muscle during inspiration.

shows excellent diagnostic accuracy in diagnosing pleural effusion, pneumothorax, pulmonary venous congestion and consolidation [31–33].

In the diagnosis of lung pathologies, we often use ultrasound artifacts, arising from the chest wall and pleural surface, as an interpretation. In order to understand the relevant normal anatomy, we will summarize the various patterns one may encounter when performing lung sonography.

Healthy lung tissue is composed primarily of air which explains why it is not routinely visualized. The air in the lung scatters and impedes the transmission of sound waves. There is a huge gap between the acoustic characteristics of soft tissues and the lung. The surface of the lung is a strong reflector of ultrasound waves and thus creates several reverberation artifacts. These artifacts contain valuable information and correlate with the current lung pathophysiology.

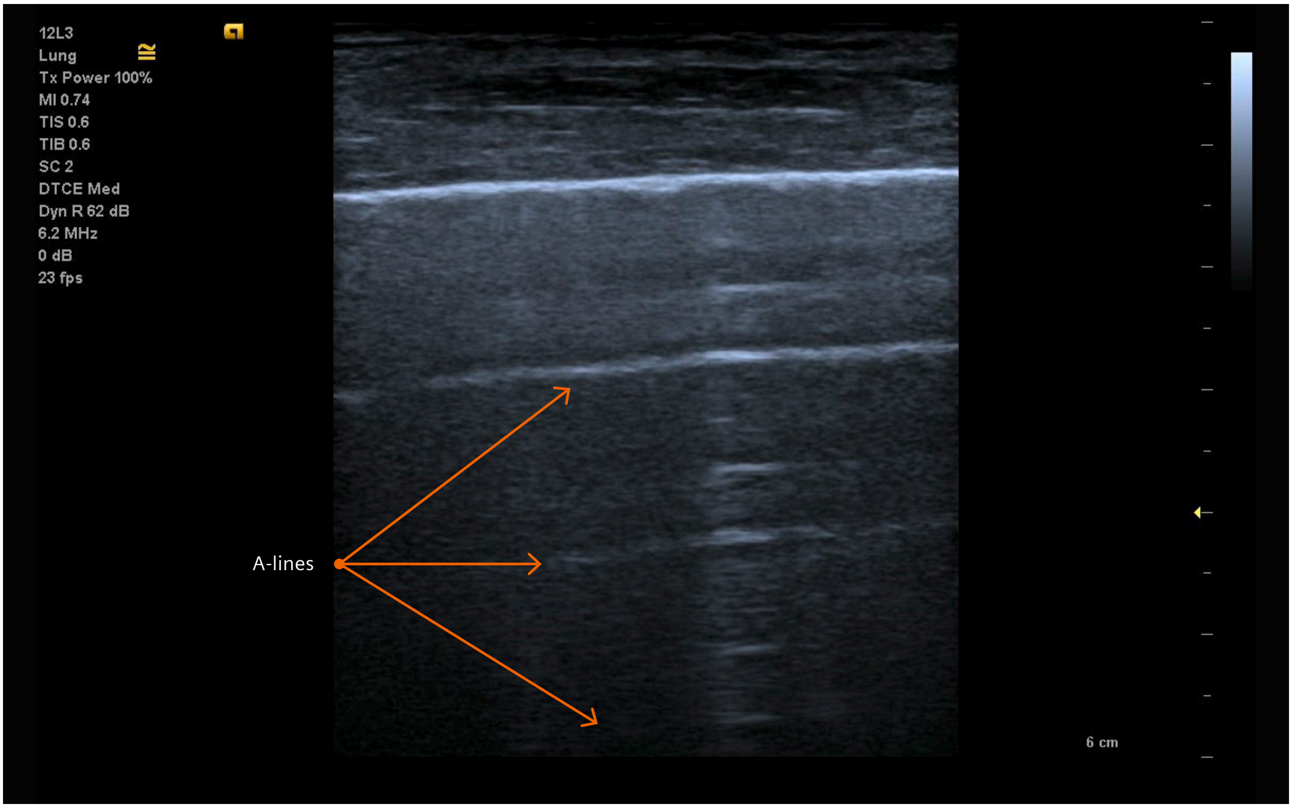

Figure 5: Ultrasound image demonstrating A-lines using a linear transducer. The A-lines are the bright horizontal lines deep to the pleural line. A-lines are a classic reverberation artifact.

Artifacts

In lung sonography we essentially interpret artifacts and use their appearance for diagnostic purposes. There are two predominant artifactual patterns that a clinician may observe, and these have been termed "A-lines" and "B-lines" [34].

A-lines

A-lines are reverberation artifacts caused by oscillating sound waves. The ultrasound waves are reflected strongly by this tissue and the air interface and reverberate [35–36]. The ultrasound waves bounce back and forth, between the transducer and lung surface. A-lines are parallel horizontal repetition lines of the pleura in the ultrasound image. Due to the fact that this is a classic reverberation artifact, the distance from the skin to the pleural line equals the distance from the pleural line to the first A-line, the first A-line to the second A-line, and so forth **(Figures 5–7)**.

The A-line is created by an intact "dry" lung parenchyma containing air combined with normal lung sliding. When sliding lung is absent, it is strongly suggestive of pneumothorax [37].

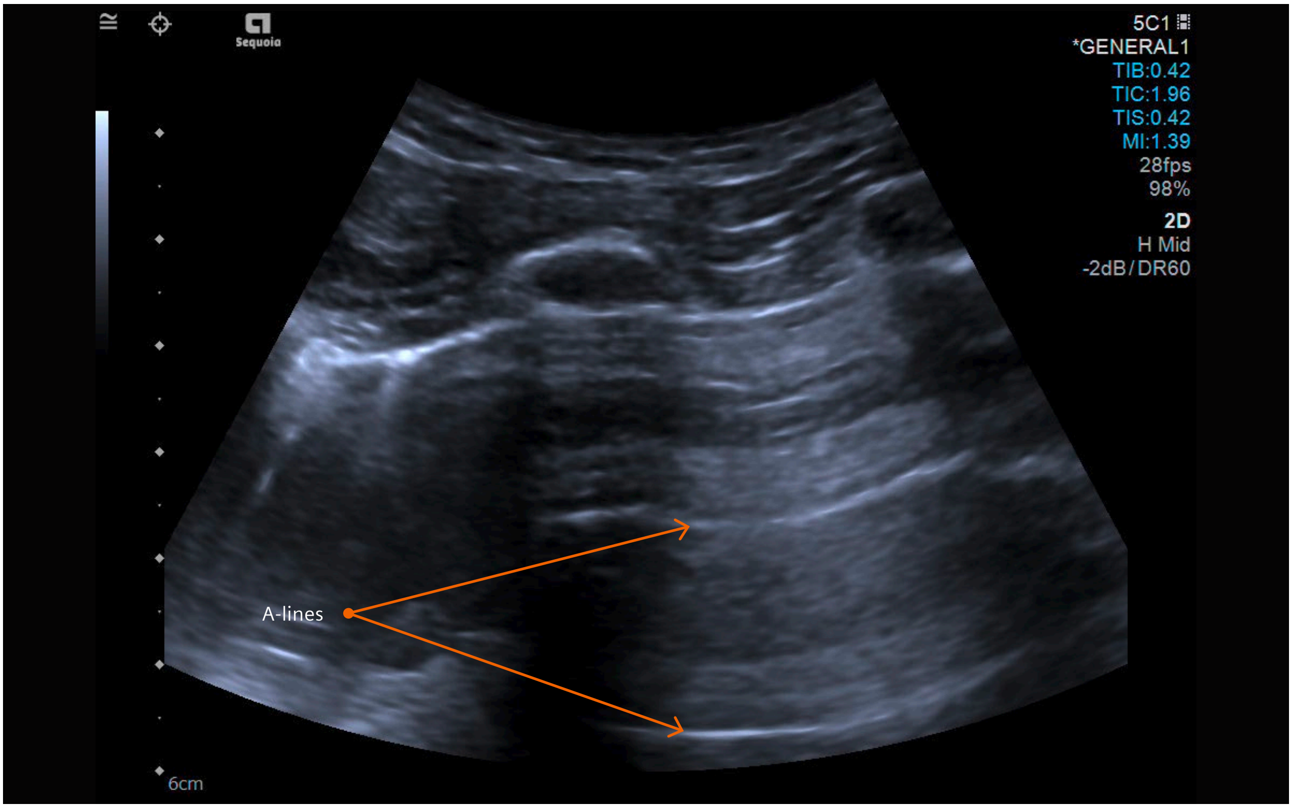

Figure 6: Ultrasound image demonstrating A-lines using a curved transducer. The A-lines are the bright horizontal lines deep to the pleural line. A-lines are a classic reverberation artefact. The distance from the skin to the pleural line equals the distance from the pleural line to the first A-line.

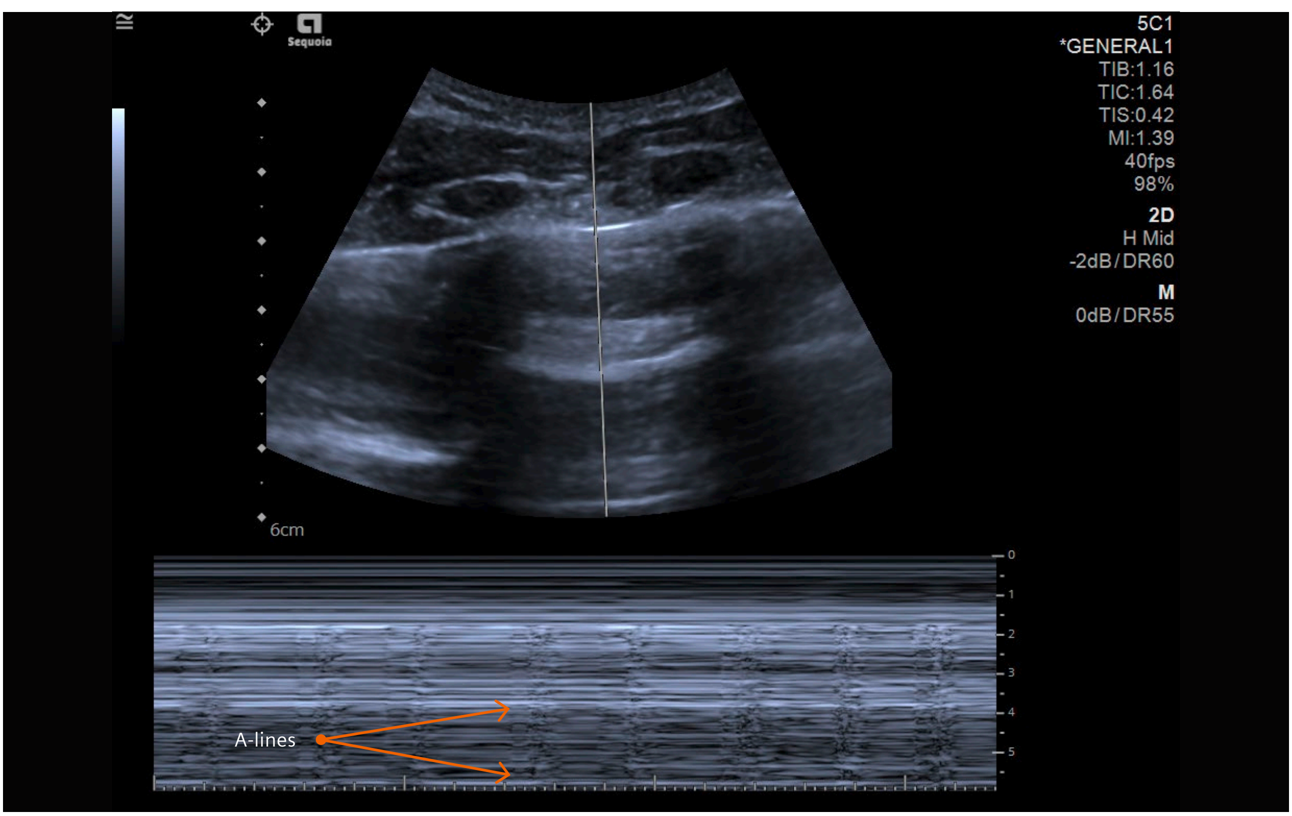

Figure 7: Ultrasound image demonstrating A-lines using a curved transducer. The A-lines are clearly visible on the M-mode as bright white lines.

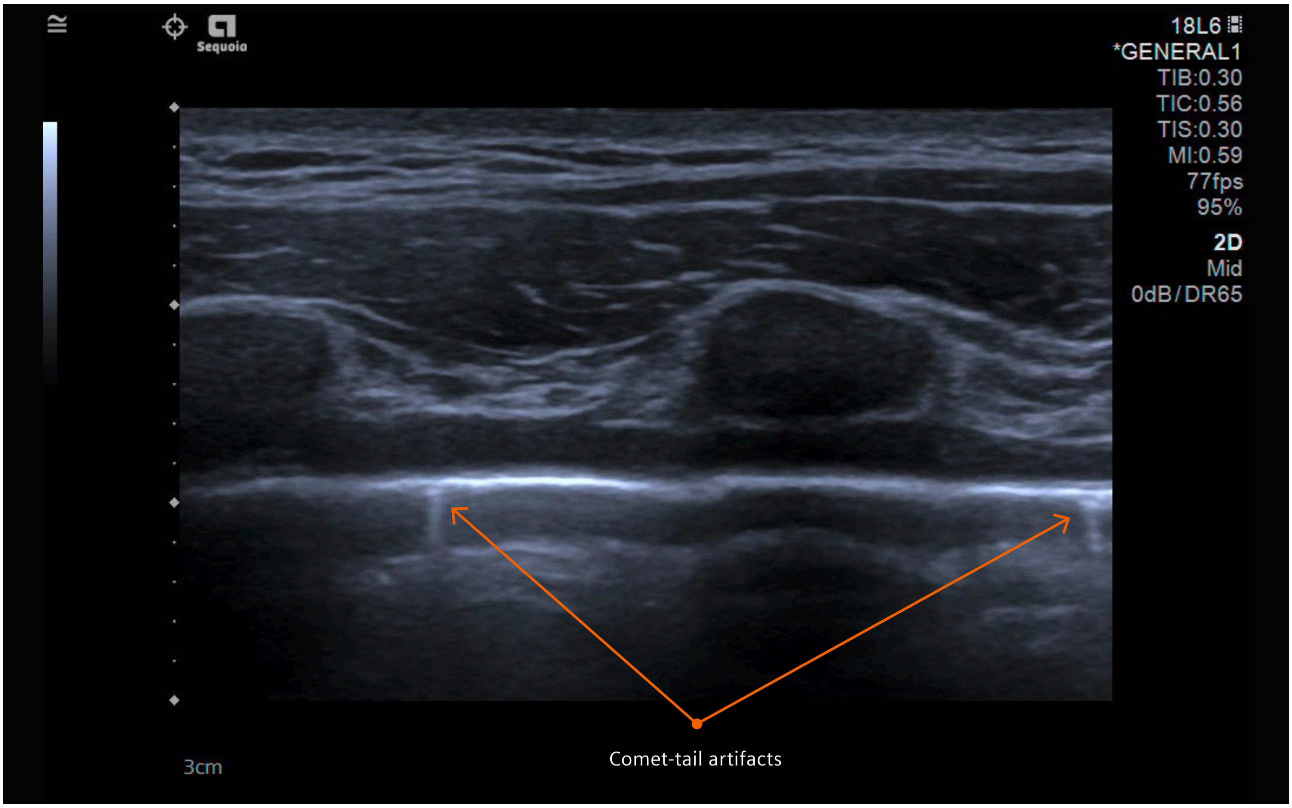

Figure 8: Ultrasound image demonstrating comet-tail artifacts. The artifact originates at the pleura but fades.

B-lines

The "comet-tail" ultrasonographic sign was first described by Ziskin and colleagues in 1982 when an intrahepatic shotgun pellet was observed to create an artifact like what is seen in lung comets [38]. B-lines are not to be confused with normal comet-tail artifacts that originate at the pleura but fade before reaching the edge of the screen **(Figure 8)**.

The B-lines are vertical, highly dynamic, hyperechoic artifacts originating from the pleura or consolidation areas [37]. These lines indicate accumulation of fluid in the pulmonary interstitial space ("lung rockets") or alveoli ("ground glass"). Multiple B-lines are associated with pulmonary edema of cardiogenic and noncardiogenic or mixed origin. They occur when sound waves pass through the superficial soft tissues and cross the pleural line encountering a mixture of air and water. One or two B-lines are not too concerning but when they increase in number or spread out in one zone, they are an indication of lung interstitial syndrome **(Figures 9–10)**.

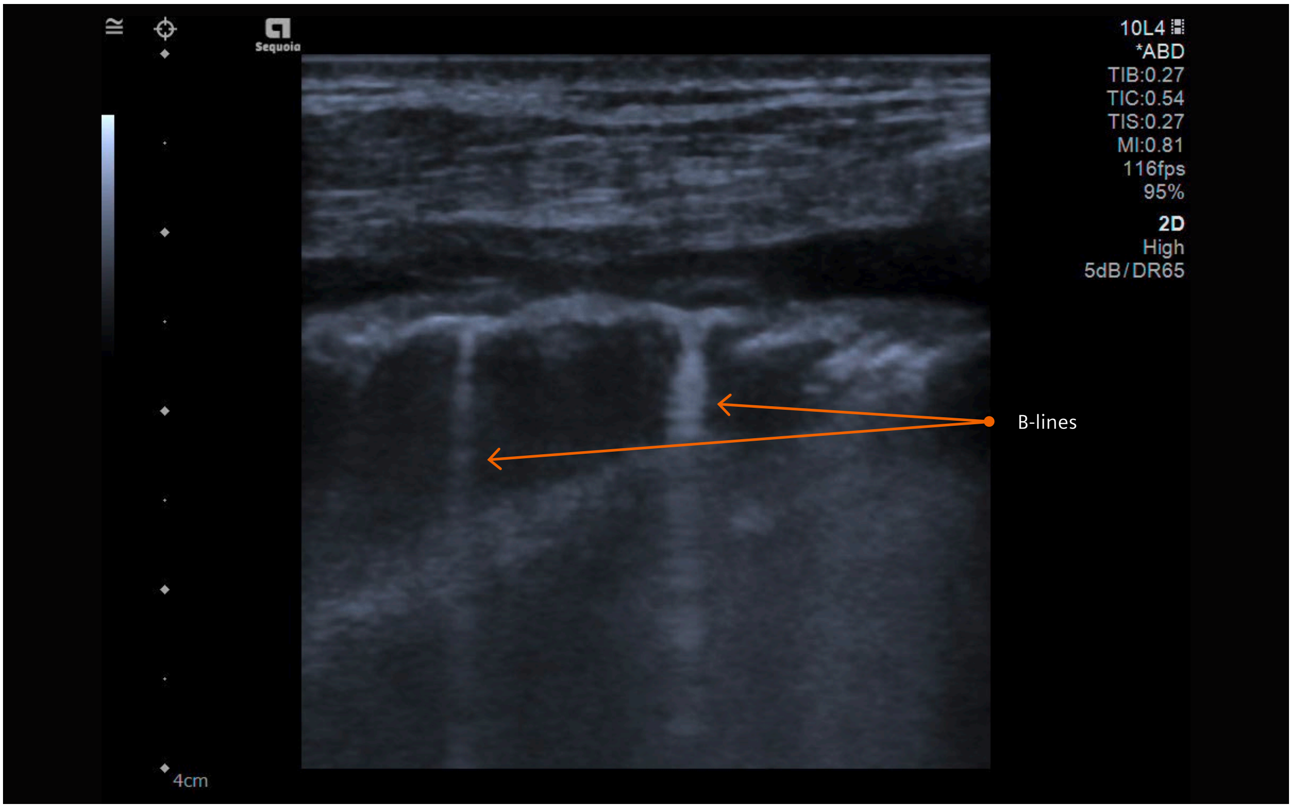

Figure 9: Examination of the lung using a linear transducer. B-lines are discrete vertical hyperechoic reverberation artifacts that arise from the pleural line and extend to the bottom of the screen without fading. These artifacts move synchronously with lung sliding.

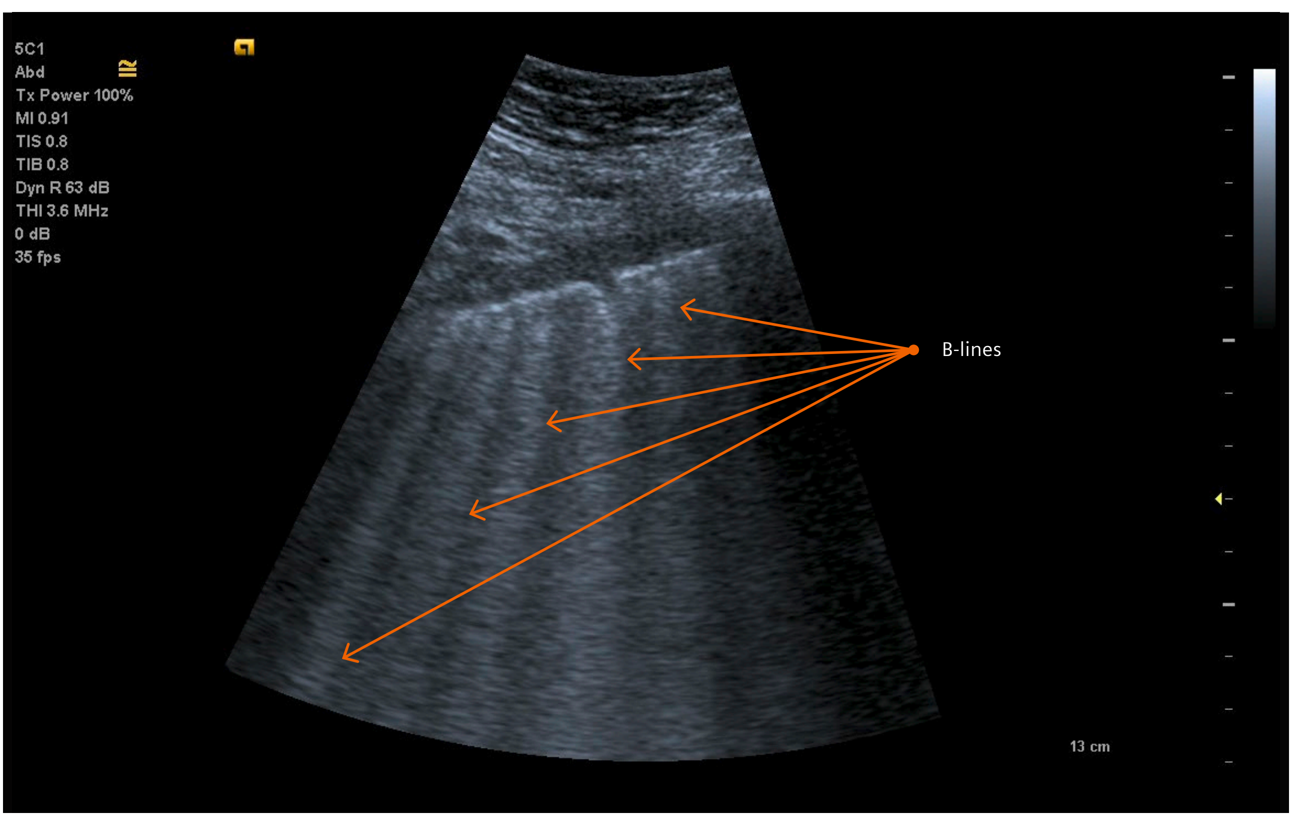

Figure 10: Examination of the lung using a curved transducer. B-lines are seen arising from the pleural line and extending to the bottom of the screen without fading.

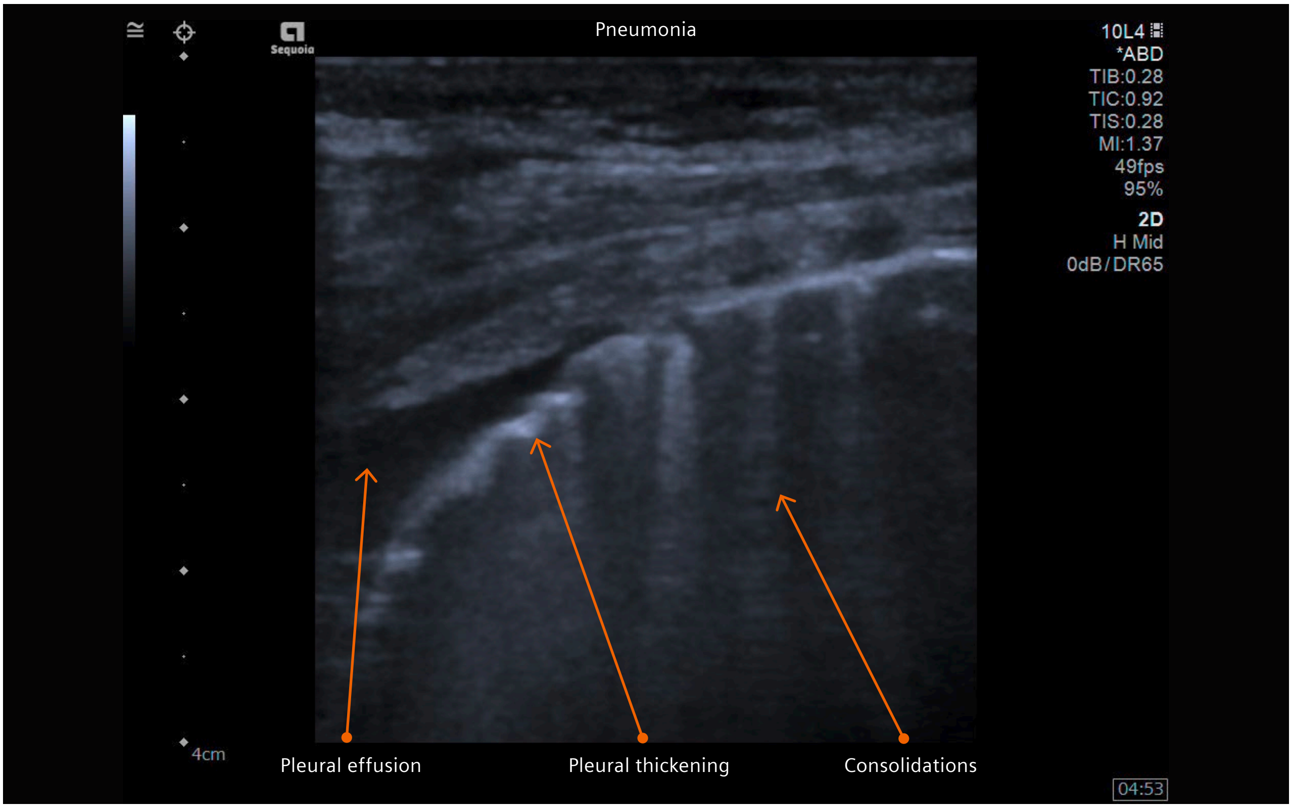

Figure 11: Pneumonia examination of the lung with a linear transducer. Ultrasound findings including pleural effusion, pleural thickening and consolidations with additional accompanying B-line artifacts are seen.

Transducer selection and settings

Lung ultrasonography often relies on analysis of artifacts, such as A and B-lines, which can be optimized by altering machine settings; the experienced operator adapts machine settings for optimal visualization of these artifacts [39]. Conventional ultrasound systems with a "real-time B-mode" technique are suitable for preoperative and postoperative transthoracic ultrasound. Several ultrasonography probes are used for lung ultrasound (LUS), and each has specific advantages and limitations. The choice generally depends on multiple factors, including patient anatomy, size and age, the depth and nature of the visualized structures and the goals of the investigation. Low-frequency convex transducers are more suitable for Bedside Lung Ultrasonography (BLUE) because they can be used to visualize the deep posterior-lateral structures and can reveal consolidation and pleural effusion [37]. However, low-penetration, high-frequency and high-definition linear transducers may be preferable for identifying pneumothorax and examining the superficial anterior structures (i.e. pleural line lung sliding) in both children and thin adults. Phased and microconvex transducers can be used for a broad range of specific indications. Keep in mind that low-frequency transducers will provide more depth penetration but will sacrifice some image quality; high-frequency transducers will provide better resolution but will sacrifice depth penetration [37]. In recent years, however, prospective studies using high-frequency linear, low-frequency curvilinear and low-frequency sector transducers have demonstrated that the performance and interpretation of lung sonography is not transducer-specific [39]. We use an ultrasound system with a convex (5–1 MHz), linear (10–4 MHz) or sector transducer (8–3 MHz) **(Figure 11)**.

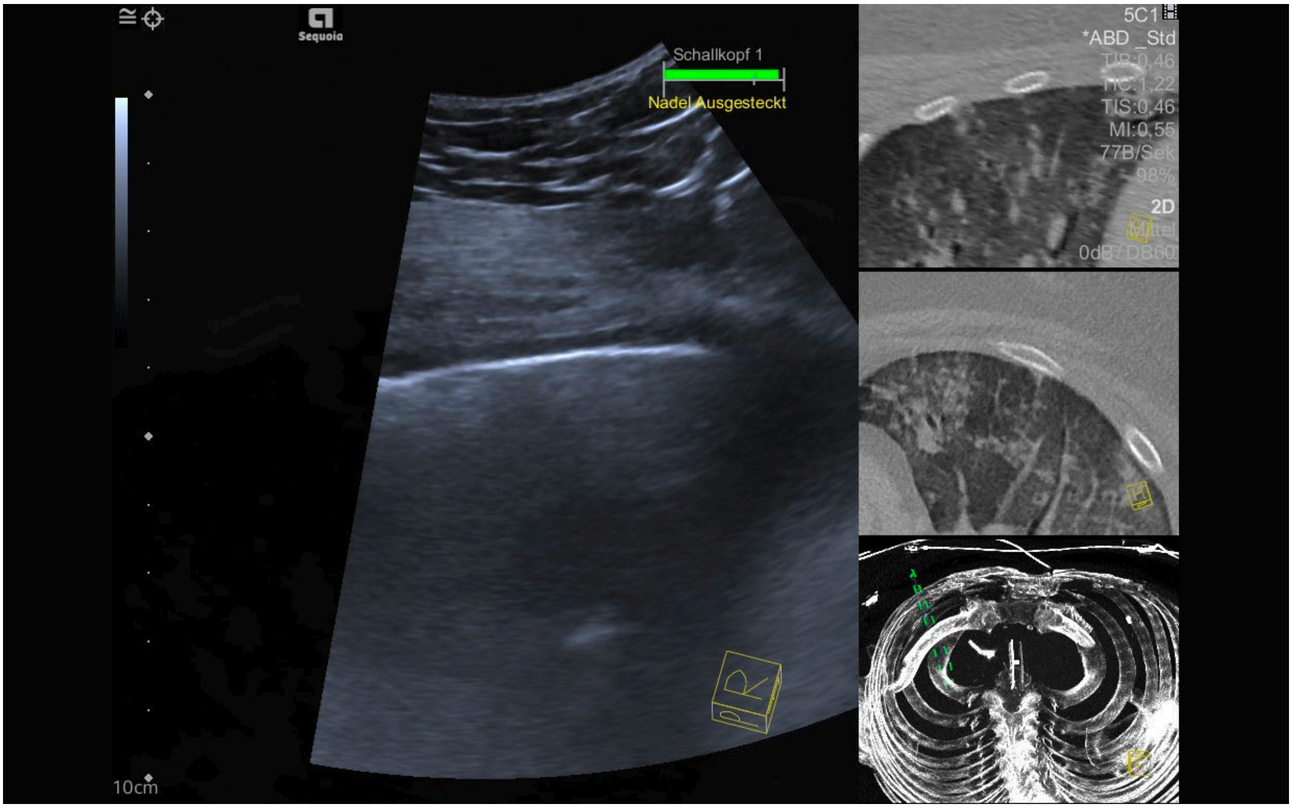

Figure 12: COVID-19 pneumonia. Follow-up examination in the ICU using real-time image fusion technique with a curved transducer. Ultrasound findings including pleural thickening and consolidations of the lung in the side-by-side mode are detected. HR-CT showed ground glass opacity and reticular shadows under the pleura in the field of the right lung.

The basic ultrasound units should be equipped with pulsed and color Doppler and M-mode to be able to evaluate vessels and the vascularization of pathological findings [40].

In addition to standard B-mode, the diagnostic value of ultrasound can be improved by using dynamic M-mode. With M-mode, a single vertical line of the ultrasound image is selected. The ultrasound signals of this line are displayed over time in a separate diagram which allows movements in the tissue to be represented as curves. Immobile structures appear as horizontal lines. When M-mode is applied to the lung exam, the system displays a representation of tissue motion over time [35].

The advanced ultrasound systems should be equipped with shear wave elastography imaging, contrast enhanced ultrasound (CEUS) and image fusion. Most ultrasound manufacturers use technical processes for image enhancement, such as Compound Imaging and Harmonic Imaging. The result of using these modes is overall better image quality necessary for a conventional examination, however, disabling these modes will result in a clearer display of comet-tail artifacts or B-lines [35].

To optimize the visualization of the pleural line, the focal zone, image depth and overall gain should be adjusted [14].

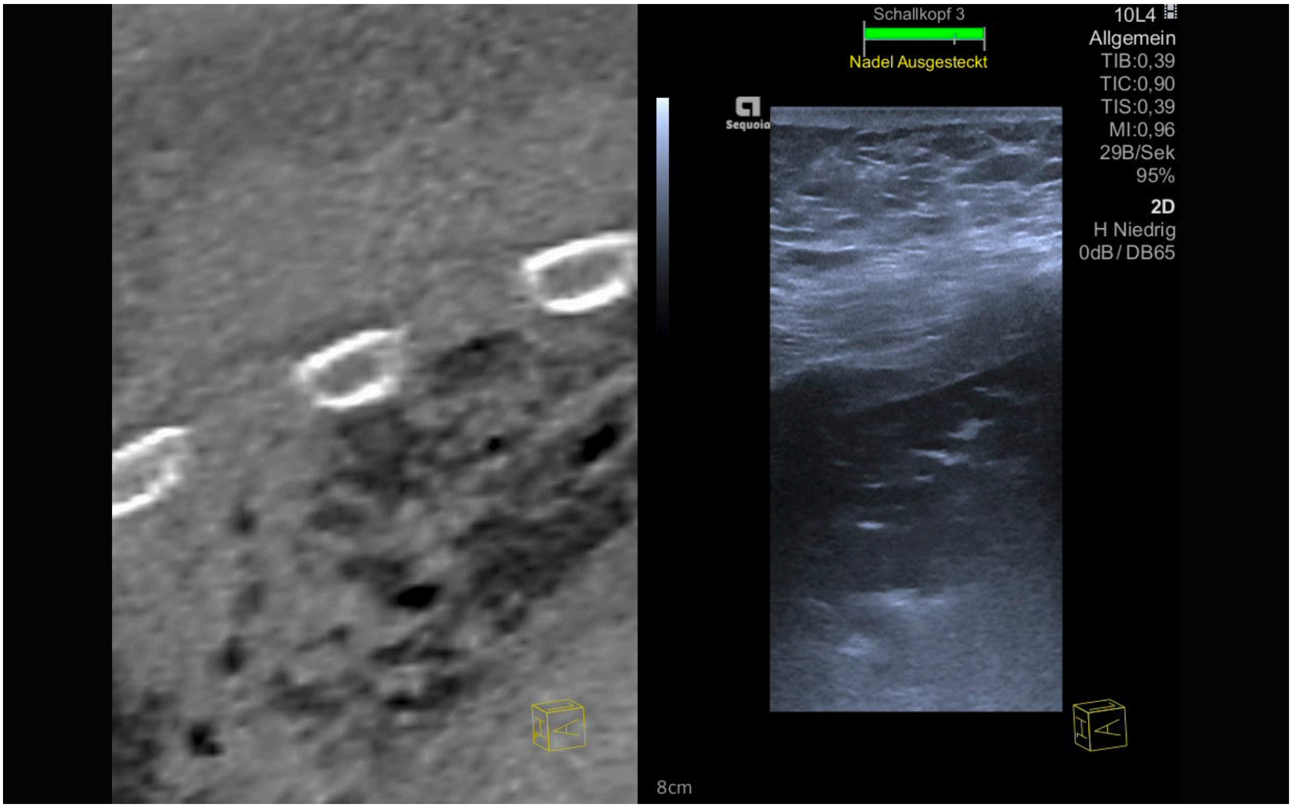

Figure 13: COVID-19 pneumonia. Follow-up examination in the ICU using real-time image fusion technique with a linear transducer. HR-CT showed large flaps of soft tissues and low-density shadows under the pleura in the posterior segment of upper lobe of the left lung, and a large air bronchogram sign confirmed by ultrasound using the image fusion technique.

Image fusion

For complicated lung pathologies, real-time ultrasound image fusion with a HR-CT dataset can be performed with high-end ultrasound systems. This is especially useful for ill patients in the ICU, because pathologies could be monitored directly at the bedside. CT examinations could be minimized and the risk for contamination due to less transportation of the patient will also decrease. When performing ultrasound fusion, there is additional hardware required that includes a magnetic field generator and a position sensor. The position sensor makes it possible to detect the position of the transducer in the three-dimensional space. Image fusion is possible with most imaging modalities including CT. DICOM (digital imaging and communication in medicine) datasets of HR-CT scans can be coregistered with the help of the ultrasound system software and can be viewed in a side-by-side mode or in an overlay mode in real-time [42] **(Figures 12–13)**.

During image fusion, it is still technically possible to use all other image modes of the ultrasound system such as color Doppler and CEUS. Using multiple image techniques in real-time allows comprehensive imaging and characterization of the vascularization of lung pathologies [43]. Fusion imaging could help in the detection and localization of lung lesions with low conspicuity on standard B-mode ultrasound. In abdominal imaging and animal studies, image fusion is already being used on several organs [44–64].

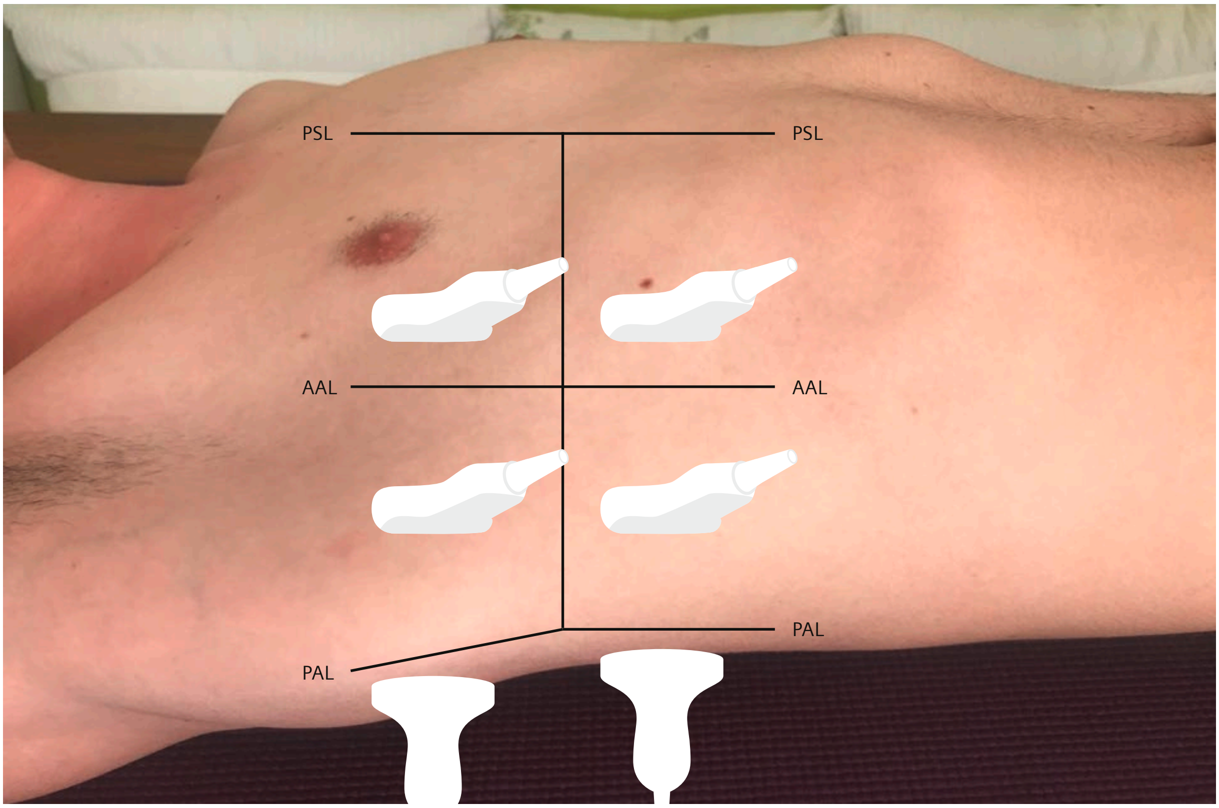

Figure 14: Transducer positions for a lung ultrasound examination in the recumbent/supine patient. The abbreviated examination covers two BLUE points and the PLAPS (posterolateral alveolar and/or pleural syndrome) points on both sides (for the detailed description and how to localize BLUE and PLAPS points see [72]).

Examination procedure

Lung ultrasound is used in emergency and intensive care patients in supine (ventral thorax) and, depending on the clinic, in a sitting position (dorsal thorax). The exam should be performed in a systematic manner that investigates the entire anterolateral and posterior lung surfaces bilaterally, or when indicated, can be performed with a patient-focused abbreviated approach. Typically, the transthoracic scanning window will be used for the examination of the lung and pleura [36]. The intercostal spaces serve as scanning windows. The transducer should be positioned at right angles to the ribs so that two adjacent ribs are captured. This allows the lung to slide, i.e. the movement of the pleura visceralis, reliably identified and from the anterior rib artifact can be distinguished. By using these techniques, each intercostal space of upper and lower parts of the anterior, lateral, and posterior regions of the left and right chest wall will be carefully examined [65].

Three "standard" lung points are usually described in relation to the Bedside Lung Ultrasonography (BLUE) protocol and include the upper, lower, and posterior-lateral alveolar pleural syndrome views. However, it is important to note that the BLUE protocol was developed for hypoxemic patients to improve the diagnostic tree quality and avoid false negative results, without undue modification of the treatment plan [66]. In addition, three conventional anatomic areas (anterior, lateral, and posterior) can be identified at each hemithorax by using the anterior and posterior axillary lines as landmarks [37]. In Austria, Switzerland and Germany we have adopted a modified BLUE point protocol for COVID-19 patients to include 6 additional views **(Figure 14)**.

Figure 15: CT-Topogram of a lung detected a pneumothorax on the right side which was afterwards treated with a Bülau-Drainage.

Basic lung exam

By using lung ultrasound, the following clinical indications should be excluded or confirmed. Pleural effusion, pulmonary edema/interstitial syndrome, atelectasis, pneumonia and pneumothorax [67]. The diagnosis of peripheral pulmonary embolisms is possible, but it is usually very time-consuming, because the complete lung must be systematically examined. Ultrasound guided thoracentesis allows for direct visualization of the drain placement and additional follow-up as clinically necessary.

Pneumothorax

Lung ultrasound is a sensitive and specific technique for identifying pneumothorax, including the occult form, and for guiding chest drainage as an emergency life-saving procedure. The diagnosis of pneumothorax traditionally has been based on chest radiography. Although up to 50% of cases can only be detected using HR-CT, that is not the case using plain chest radiography because of anterior air collection [68]. In this setting, lung ultrasound provides much better accuracy for the early detection of pneumothorax. A large meta-analysis study revealed that lung ultrasound provided better sensitivity than plain chest radiography (91% v 50%) with similar specificity for pneumothorax (98% v 99%) [37, 69–70] **(Figures 15–16).**

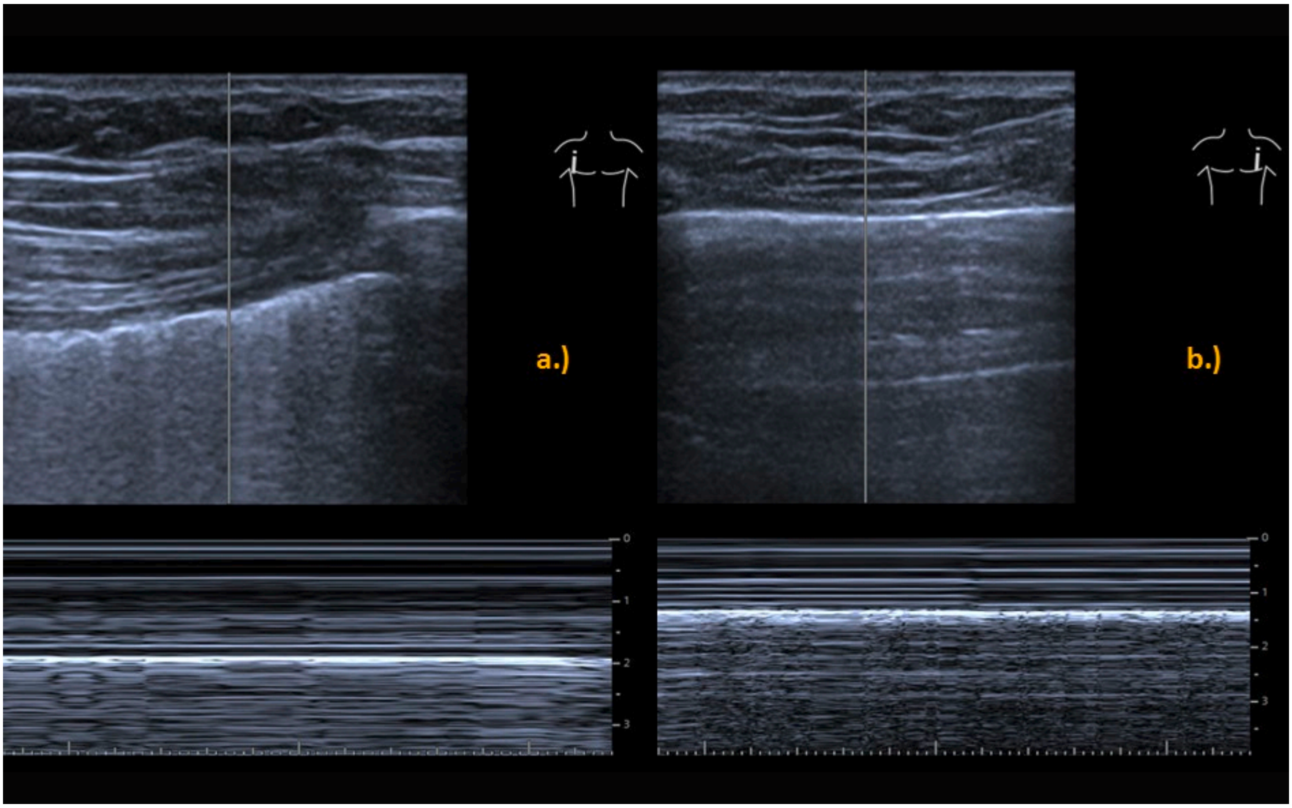

Figure 16: Follow-up examination of the same patient two days later in the ICU. In M-mode (a.), the absence of motion is documented as a static pattern of horizontal lines ("stratosphere sign"). In comparison to the M-mode (b.), the seashore sign is clearly visible.

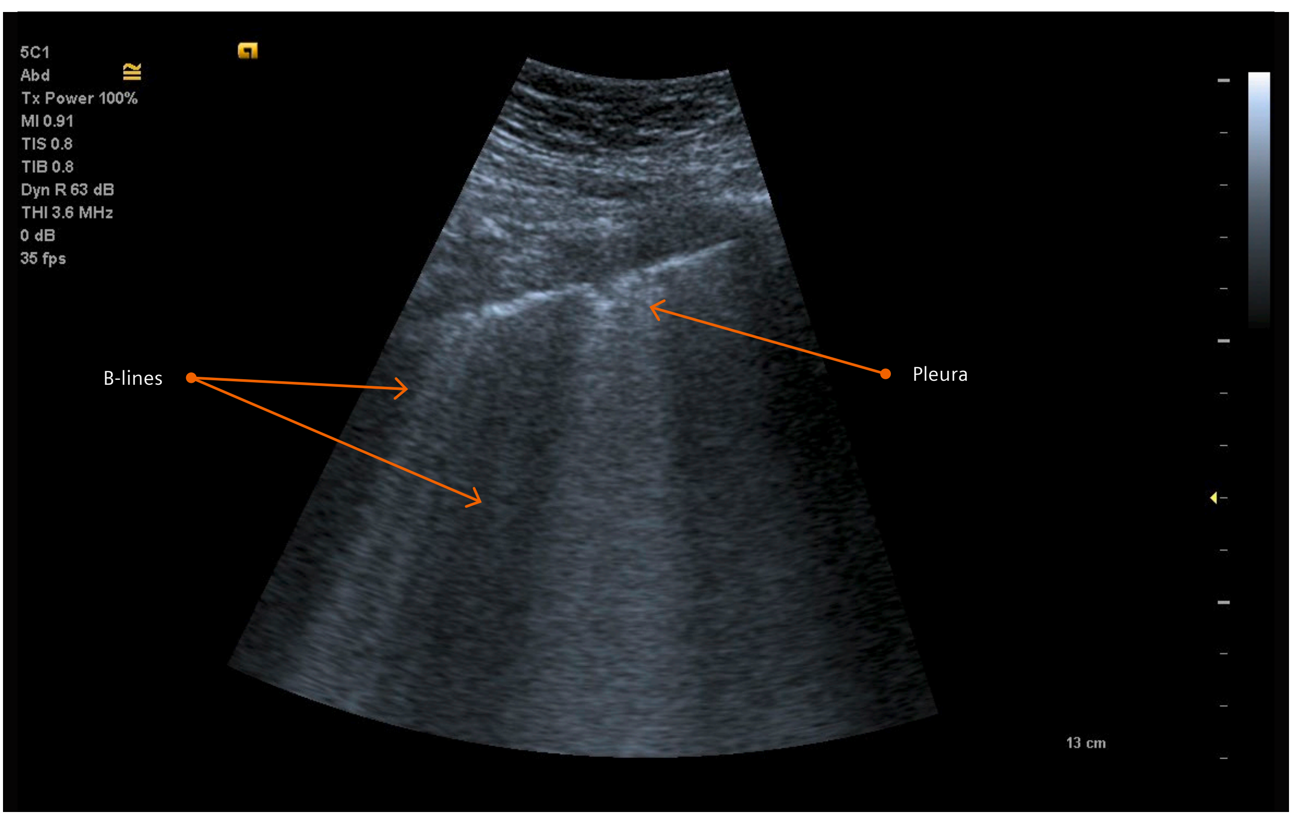

Figure 17: COVID-19 pneumonia. Follow-up examination in the ICU using a curved transducer. Ultrasound findings including pleural thickening and irregularity. Additionally, consolidations of the lung with B-lines are detected.

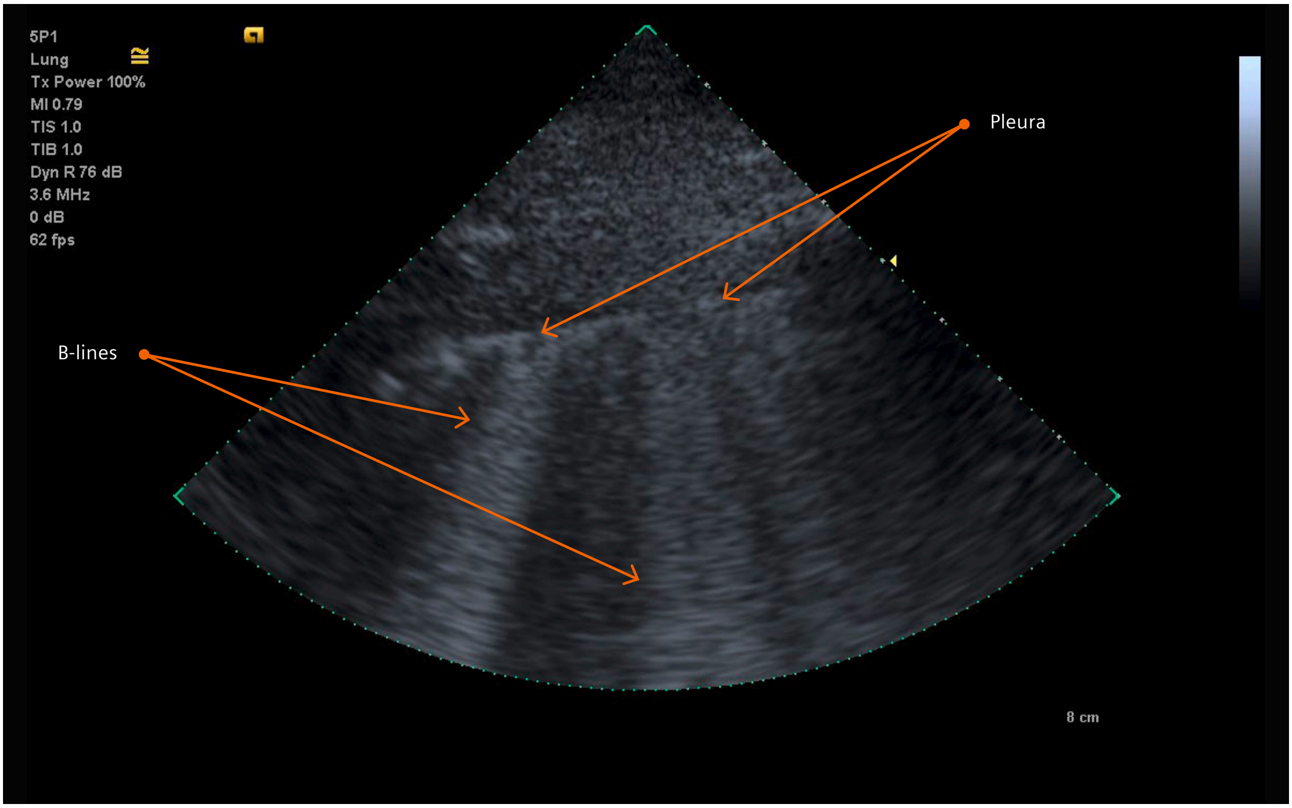

Figure 18: COVID-19 pneumonia. Follow-up examination in the ICU using a sector transducer. Ultrasound findings including pleural thickening and irregularity. Additionally, consolidations of the lung with B-lines are detected.

Pneumonia

Pneumonic infiltrates can be visualized by ultrasound if they are close to the pleura. Central lung pneumonia could not be detected. In critically ill patients, pneumonia usually spreads to the periphery, so that it can be easily detected by lung ultrasound [30, 66] **(Figures 17–18)**.

B-line artifacts are often seen in the areas adjacent to the consolidation, likely as an expression of inflammatory perilesional edema. Pleural line abnormalities and pleural effusions were consistently associated with areas of confluent B-line artifacts and/or lung consolidation [39, 71].

Sonographically, in pneumonia, the lungs typically exhibit two key ultrasound signs, B-lines and consolidation [72–73]. The pneumonic infiltrate presents itself as low-echo structures with irregular borders and inhomogeneous echo texture [74].

Reissig et al. conducted a prospective, multi-center study on the accuracy of lung ultrasound in the diagnosis and follow-up of community-acquired pneumonia [75]. In 362 patients in 14 centers, lung ultrasound had a sensitivity of 93.4% and a specificity of 97.7% for pneumonia compared to the reference of final clinical diagnosis. Breath-dependent motion of infiltrates was seen in 97.6% of the cases, an air bronchogram in 86.7%, blurred margins in 76.5% and a basal pleural effusion in 54.4% [72, 75]. Meta-analyses confirmed that pneumonia can be diagnosed using lung ultrasound [16, 76] **(Figure 19)**.

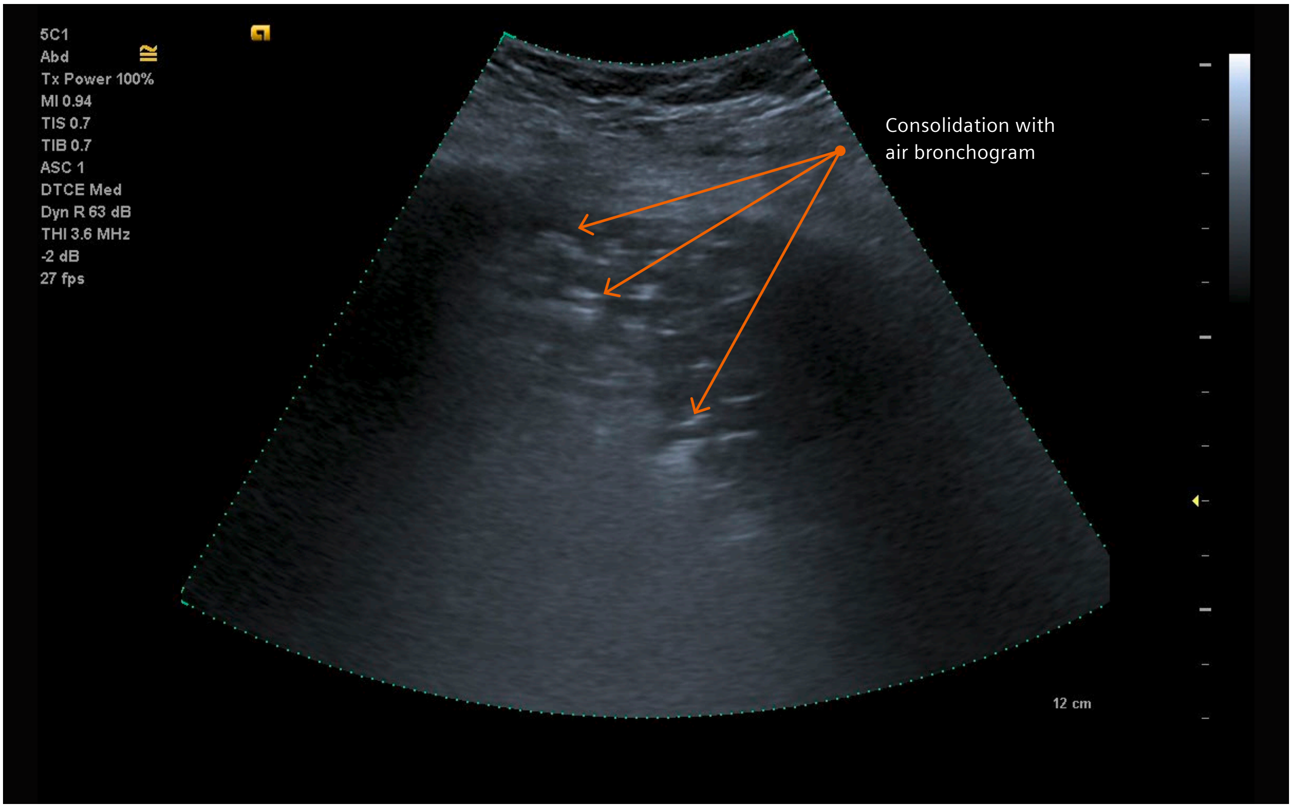

Figure 19: COVID-19 pneumonia. Follow-up examination in the ICU using a curved transducer. Ultrasound findings showed large areas of consolidation in the left posterior upper area and an air bronchogram sign.

Atelectasis

Lung atelectasis is common after cardiac surgery, with a reported incidence of up to 88% [77]. The lung sliding sign may be absent in these cases because the alveoli are not ventilated, which is associated with decreased lung volume and an upward displacement of the diaphragm dome [37] **(Figure 20)**.

The echogenicity of a complete atelectasis of the lungs looks very similar to liver tissue [72]. Ultrasound could detect small hyperechoic areas in the bronchioles which present a trapped partially air-filled area [35].

Pleural effusion

The sonographic examination of pleural effusions has already been established as a routine method since the sixties [30]. The most sensitive method for detecting pleural effusion is transthoracic ultrasound [78–79]. With the transducer in sagittal position to the ribs, pleural effusion appears in a quadrangular space defined by the pleural line (chest wall), the shadows of the ribs and the lung line (visceral pleura) – also called “quad sign” [72] **(Figures 21–22)**.

The effusion volume (V) in milliliters could be measured with the simplified formula. The formula contains maximum effusion height (ME [cm]) and the measurement of the basal diaphragm-lung distance (DL [cm]) [80].

(V [ml] = (ME [cm] + DL [cm]) x 70)

It measures only a rough estimate of the effusion volumes, since the variable geometric shape during respiration. With larger pleural effusions, it is often possible to develop compression atelectasis.

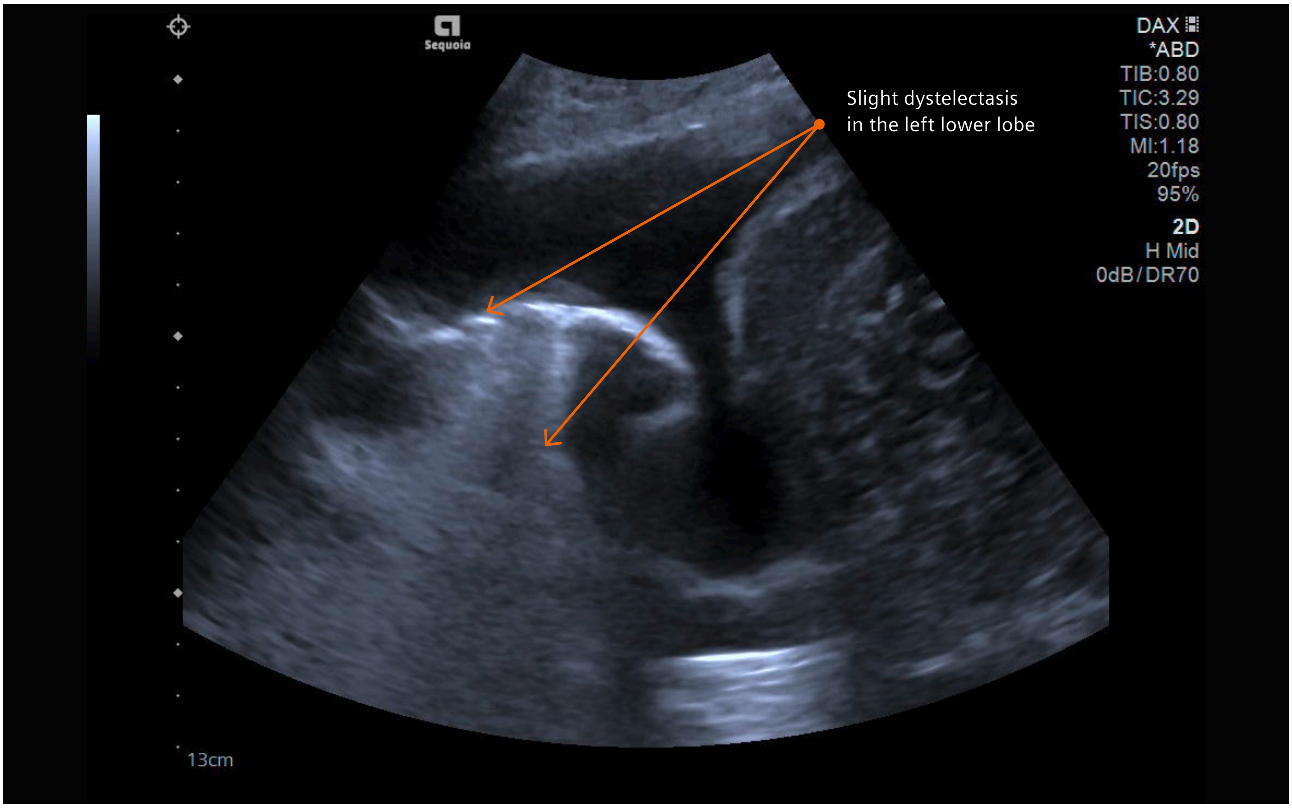

Figure 20: Pleural effusion and slight dystelectasis of the left lower lobe.

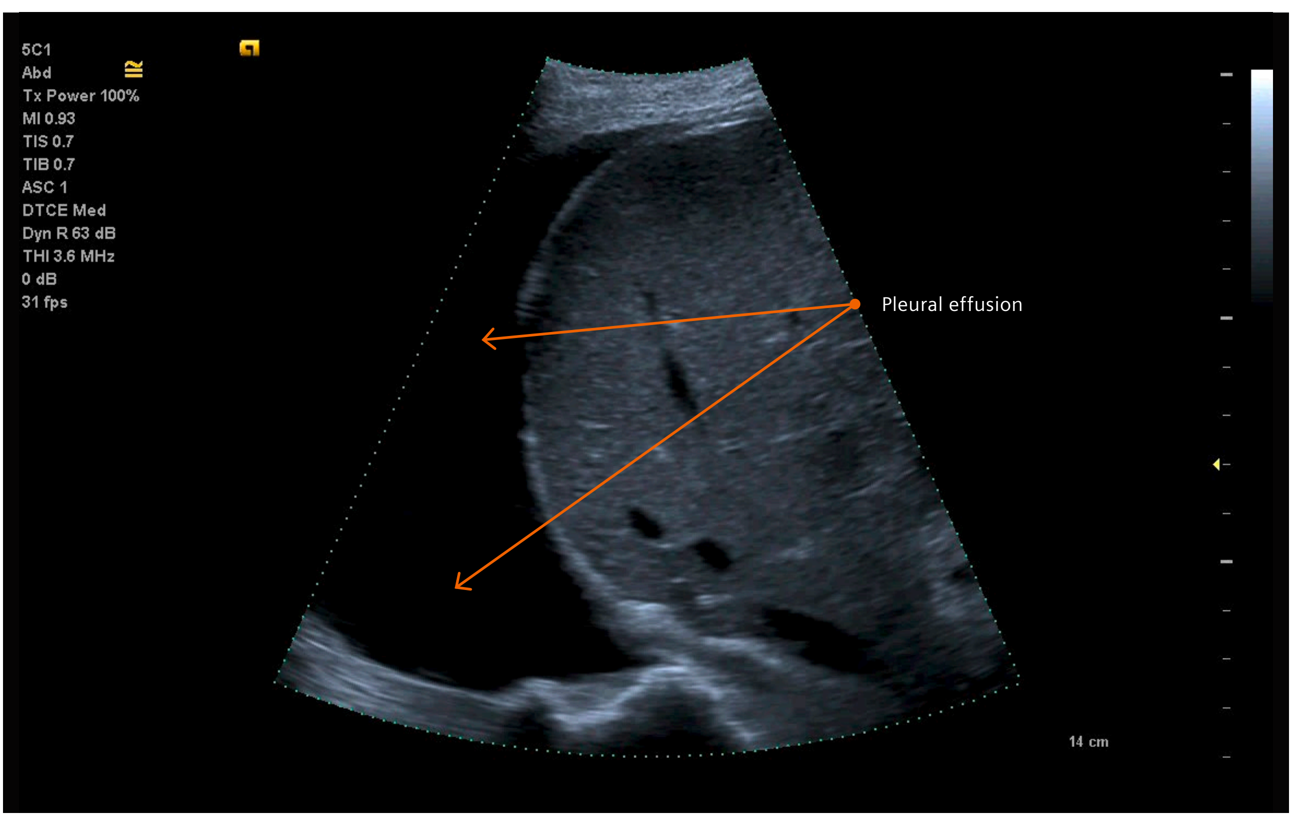

Figure 21: Pleural effusion right side.

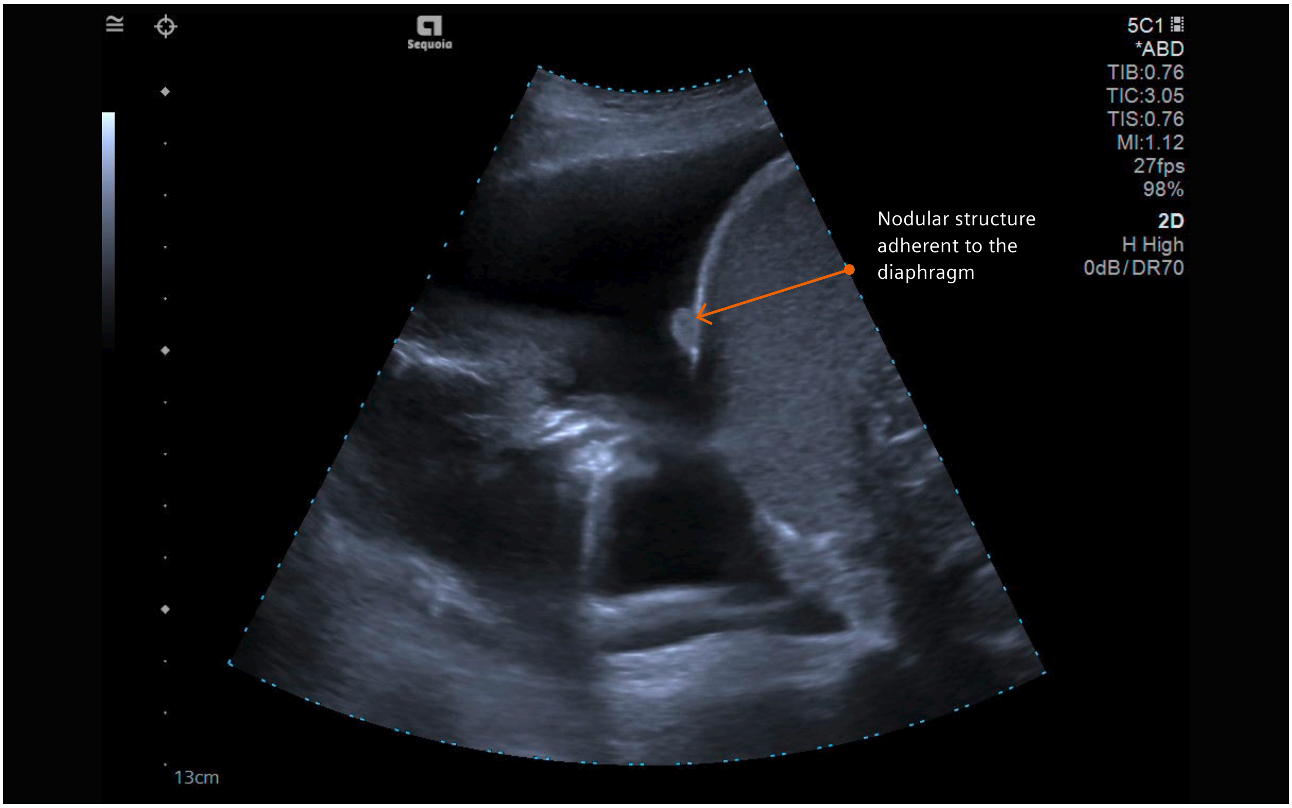

Figure 22: Pleural effusion left side and adherent nodular structure to the diaphragm is detected.

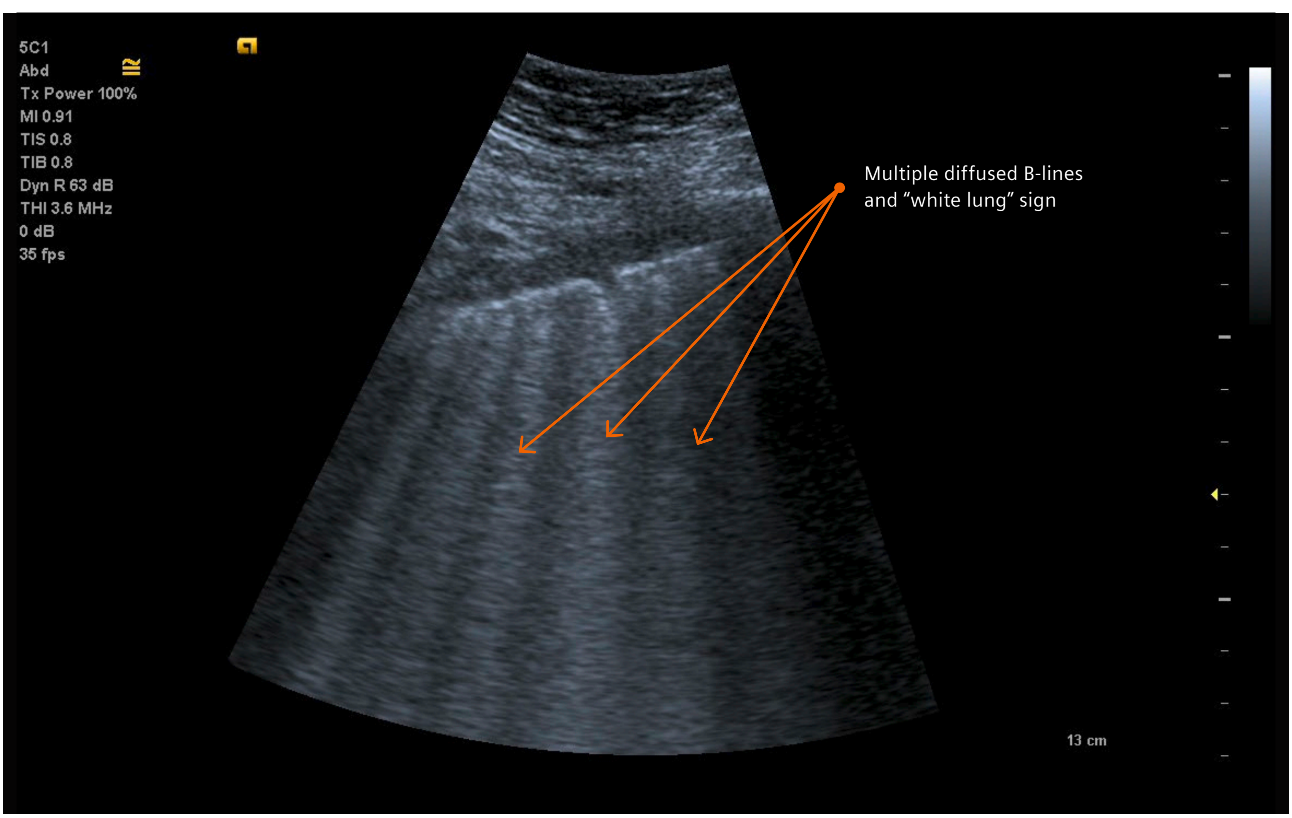

Figure 23: COVID-19 pneumonia. Follow-up examination in the ICU using a curved transducer (5–1 MHz). Ultrasound findings including pleural thickening and irregularity. Additionally, consolidations of the lung with B-lines are detected.

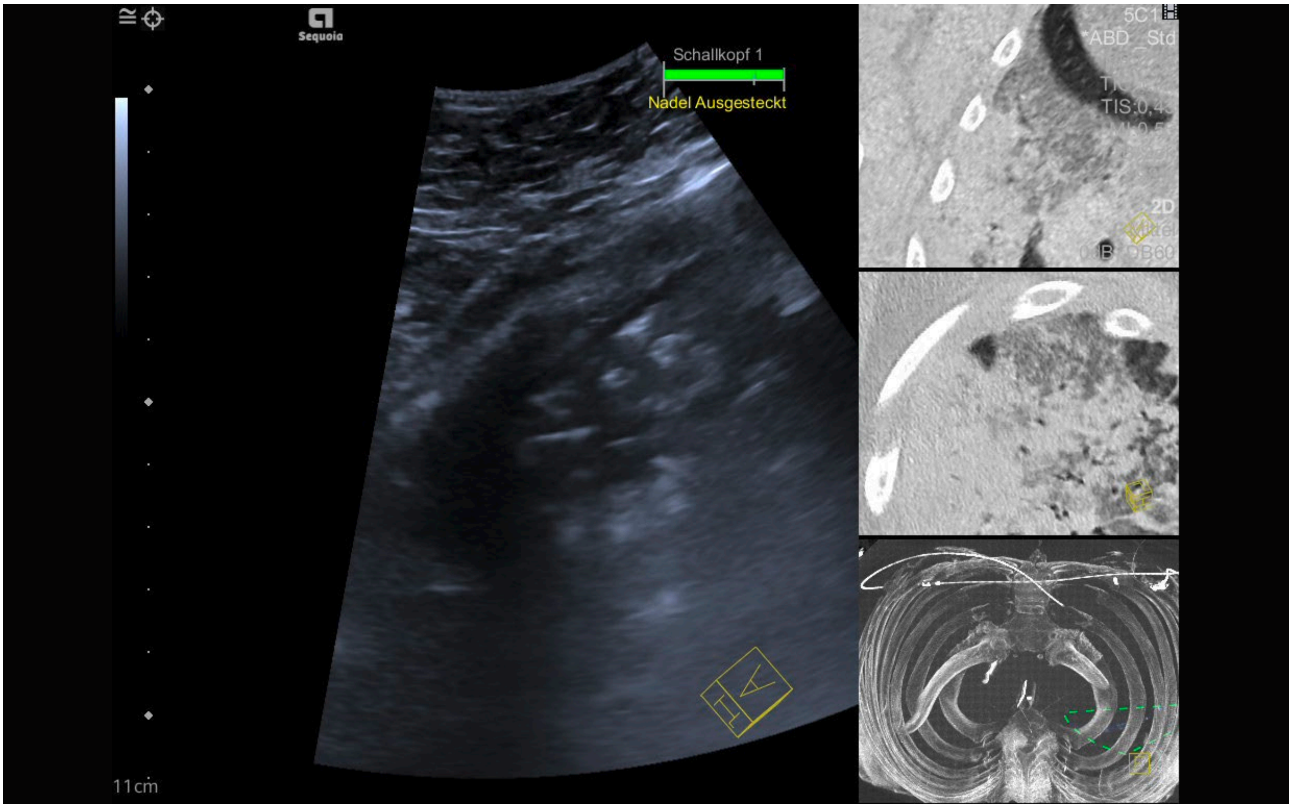

Figure 24: COVID-19 pneumonia. Follow-up examination in the ICU using a curved transducer (5–1 MHz) and the image fusion technique. Ultrasound findings showed large areas of consolidation and an air bronchogram sign.

Summary of Coronavirus COVID-19 examination and follow-up

In comparison to pneumonia caused by influenza virus, the COVID-19 virus is characterized by rapid transmission with a high infection and high lethality rate [81–83]. In comparison between non-COVID-19 pneumonia and COVID-19 pneumonia, COVID-19 pneumonia is more likely to have a peripheral distribution [84] **(Figure 23)**.

In addition to HR-CT scan and X-ray of the lung, ultrasound can also be used for the diagnosis and follow-up of the disease [85].

By using a curved transducer (5–1 MHz), the morphology and changes of subpleural lesions are clearly displayed. Due to the option to use even the low-frequency of the transducer, changes of air and water contents in consolidated peri-pulmonary tissues and an air bronchogram sign can be depicted **(Figure 24)**.

The blood supply and lesion progression in peri-pulmonary consolidation can be monitored by using the color or power Doppler technique [86].

Currently, ultrasound of the lung is limited in the diagnosis and treatment of central lung diseases due to the attenuation of sound waves by normal lung and bone tissues. The diagnosis of lung pathologies relies on the artifacts of peri-pulmonary lesions [87–88].

The artifacts exist because of an abnormal ratio of air and water contents in alveoli and interstitial tissues. In order to improve the diagnostic ultrasound lung tool, the use of an abdominal curved array probe (5–1 MHz) seems to be helpful. Typical for the COVID-19 disease are the thickening of the pleural line with pleural line irregularity. The pleural line could be unsmooth, discontinuous and interrupted [85, 89] **(Figures 25–26)**.

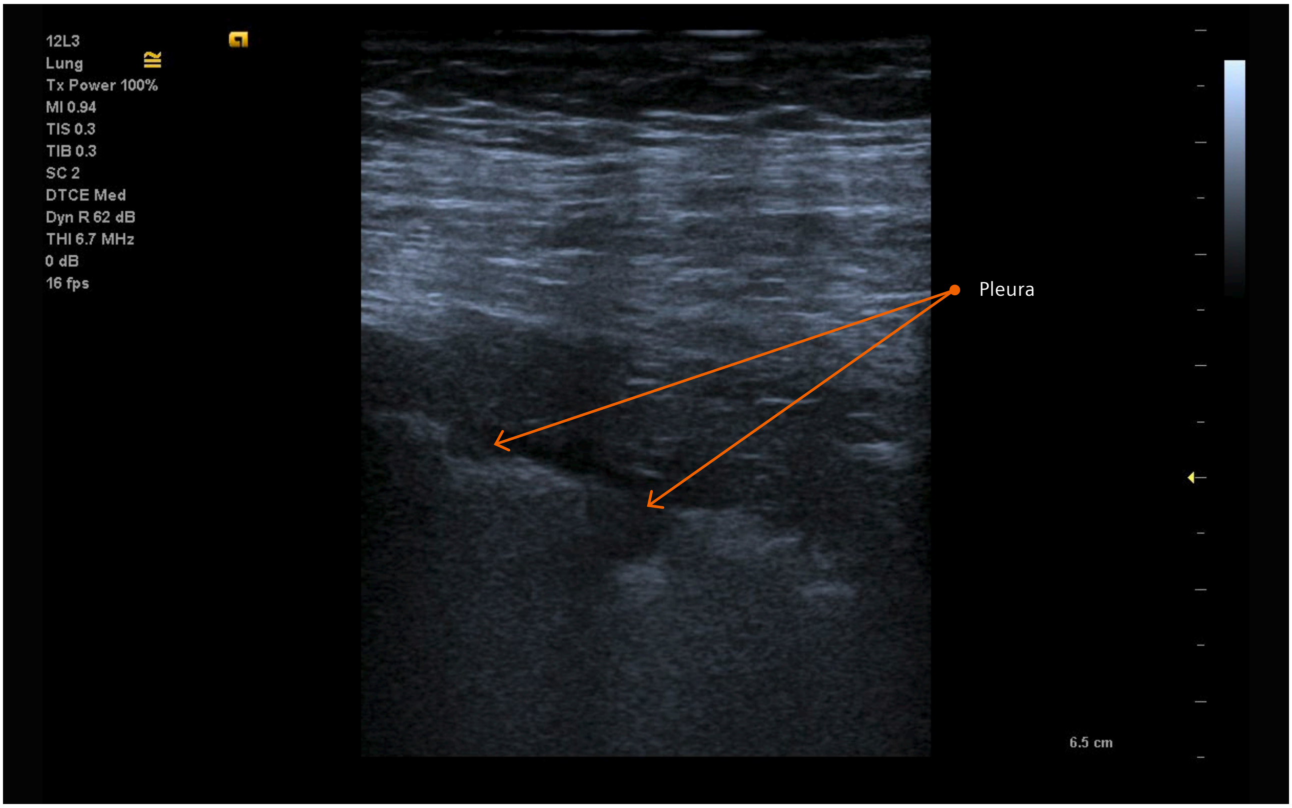

Figure 25: COVID-19 pneumonia. Follow-up examination in the ICU using a linear (12–3 MHz) transducer. Ultrasound findings including pleural thickening and irregularity are seen.

The appearance of B-lines artifacts could vary from focal, to multifocal and confluent pattern. The consolidations could vary in different patterns, including multifocal small subpleural consolidations up to non-translobar and translobar with occasional air bronchograms [5]. Pleural effusions are uncommon in coronavirus COVID-19 disease. An indirect sign for recovering is the appearance of A-lines during the recovery phase [85] **(Figure 27)**.

In summary, in our experience, we consider that lung ultrasound will have a major utility for the management of COVID-19 pneumonia in the ICU due to its safety, repeatability, low cost and point of care use. HR-CT may be reserved in the follow-up if lung ultrasound is not able to answer the clinical question. In our personal experience lung ultrasound could be used for rapid assessment of the severity of SARS-CoV-2 pneumonia, to track the evolution of disease during follow-up and to monitor lung recruitment maneuvers. Additional ultrasound can track the response to prone position and the management of extracorporeal membrane therapy [85]. With increased use of bedside ultrasound in the ICU, patients can be protected from unnecessary radiation and therapy delays. The transport of high-risk patients to X-ray examinations can be avoided.

A special thanks to my colleague for her support:

Ines Schroeder, MD
Department of Anesthesiology,
University Hospital, LMU Munich, Munich, Germany

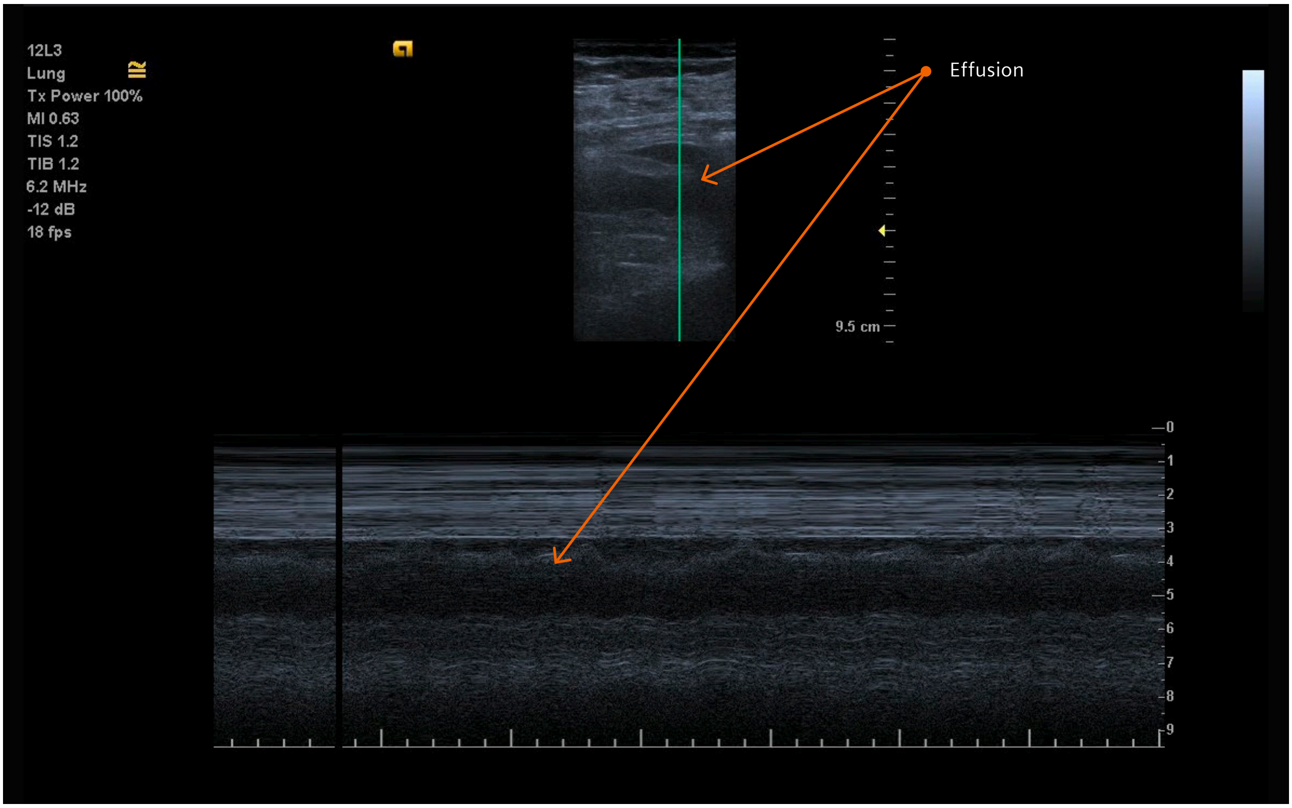

Figure 26: COVID-19 pneumonia. Follow-up examination in the ICU using a linear (12–3 MHz) transducer including M-mode and B-mode. Ultrasound findings detected pleural thickening and an additional small pleural effusion.

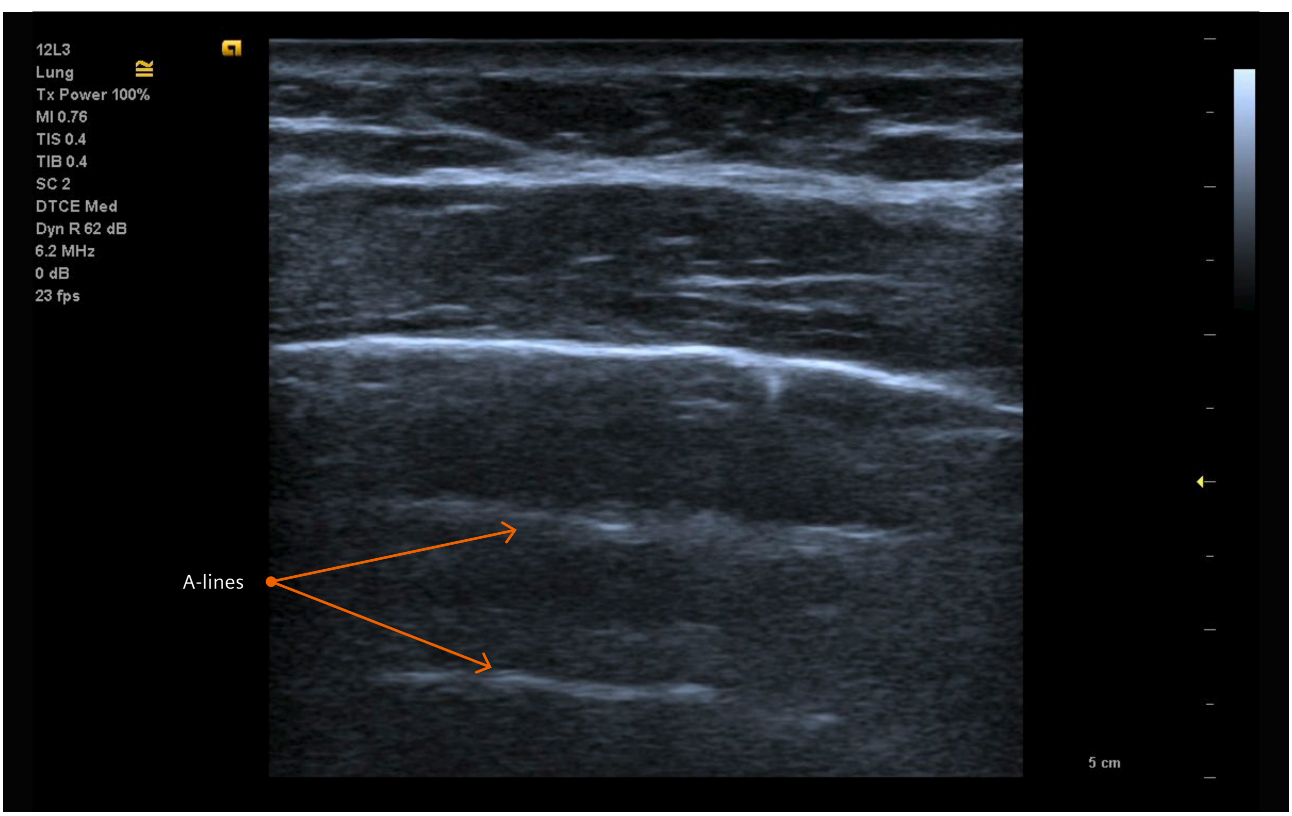

Figure 27: Follow-up after artificial respiration of COVID-19 pneumonia on a patient in the ICU. An indirect sign for recovering is the appearance of A-lines during the recovery phase.

References

1 https://coronavirus.jhu.edu/map.html

2 Cucinotta D, Vanelli M. WHO Declares COVID-19 a Pandemic. Acta Biomed. 2020 Mar 19;91(1):157-160

3 Wujtewicz M, Dylczyk-Sommer A, Aszkiełowicz A, Zdanowski S, Piwowarczyk S, Owczuk R. COVID-19 - what should anaethesiologists and intensivists know about it? Anaesthesiol Intensive Ther. 2020 Mar 20.

4 Brogi E, Bignami E, Sidoti A, Shawar M, Gargani L, Vetrugno L, Volpicelli G, Forfori F. Could the use of bedside lung ultrasound reduce the number of chest x-rays in the intensive care unit? Cardiovasc Ultrasound. 2017 Sep 13;15(1):23

5 Blaivas M, DeBehnke D, Phelan MB. Potential errors in the diagnosis of pericardial effusion on trauma ultrasound for penetrating injuries. Acad Emerg Med. 2000 Nov;7(11):1261-6

6 Oks M, Cleven KL, Cardenas-Garcia J, Schaub JA, Koenig S, Cohen RI, Mayo PH, Narasimhan M (2014) The effect of point-of-care ultrasonography on imaging studies in the medical ICU: a comparative study. Chest146:1574–1577

7 Dunn MJ, Gwinnutt CL, Gray AJ. Critical care in the emergency department: patient transfer. Emerg Med J. 2007;24(1):40–4.

8 Tecce PM, Fishman EK, Kuhlman JE. CT evaluation of the anterior mediastinum: spectrum of disease. Radiographics. 1994;14(5):973–90.

9 Brenner DJ, Hall EJ. Computed tomography–an increasing source of radiation exposure. N Engl J Med. 2007;357(22): 2277–84.

10 Tapson VF. Advances in the diagnosis and treatment of acute pulmonary embolism. F1000 Med Rep. 2012; 4:9. doi:10.3410/M4-9.

11 Lichtenstein D, Goldstein I, Mourgeon E, Cluzel P, Grenier P, Rouby JJ. Comparative diagnostic performances of auscultation, chest radiography, and lung ultrasonography in acute respiratory distress syndrome. Anesthesiology. 2004;100(1): 9–15.

12 Peng QY, Wang XT, Zhang LN; Chinese Critical Care Ultrasound Study Group (CCUSG). Findings of lung ultrasonography of novel corona virus pneumonia during the 2019-2020 epidemic. Intensive Care Med. 2020 Mar 12.

13 Mayo PH, Copetti R, Feller-Kopman D, Mathis G, Maury E, Mongodi S, Mojoli F, Volpicelli G, Zanobetti M (2019) Thoracic ultrasonography: a narrative review. Intensive Care Med 45:1200–1211.3.

14 Gargani L, Picano E. The risk of cumulative radiation exposure in chest imaging and the advantage of bedside ultrasound. Crit Ultrasound J. 2015; 7:4.

15 Volpicelli G, Elbarbary M, Blaivas M, et al. International evidence-based recommendations for point-of-care lung ultrasound. Intensive Care Med 2012; 38:577-91.

16 Volpicelli G. Lung sonography. J Ultrasound Med 2013; 32:165-71.

17 Dietrich CF, Gebhard Mathis G, Cui XW, et al. Ultrasound of the pleurae and lungs. Ultrasound Med Biol 2015; 41:351-65.

18 Mathis G. Why look for artifacts alone when the original is visible? Chest 2010; 137:233; author reply 233-4.

19 Gargani L, Pang PS, Frassi F, et al. Persistent pulmonary congestion before discharge predicts rehospitalization in heart failure: a lung ultrasound study. Cardiovasc Ultrasound 2015; 13:40.

20 Gargani L. Lung ultrasound: a new tool for the cardiologist. Cardiovasc Ultrasound 2011; 9:6.

21 Bouhemad B, Liu ZH, Arbelot C, et al. Ultrasound assessment of antibiotic-induced pulmonary reaeration in ventilator-associated pneumonia. Crit Care Med 2010; 38:84-92.

22 Buddee FW, Johnson DC, Jellins J: Experimental and clinical experiences in the use of ultrasound for the early detection of pulmonary emboli: A preliminary report. Med J Aust 1969; 1: 295–297.

23 Crawford HD, Wild JJ, Wolf PI, Finks JS: Transmission of ultrasound through living human thorax. Ire Trans Med Electron 1959; 141–146

24 Lichtenstein DA. BLUE-protocol and FALLS-protocol: two applications of lung ultrasound in the critically ill. Chest. 2015 Jun;147(6):1659-1670.

25 Weinberger SE, Drazen JM. Diagnostic procedures in respiratory diseases. In: Kasper DL, Braunwald E, Fauci AS, Hauser SL, Longo DL, Jameson JL, eds. Harrison's Principles of Internal Medicine. 16th ed. New York, NY: McGraw-Hill; 2005: 1505 - 1508.

26 Mayo PH, Beaulieu Y, Doelken P, et al. American College of Chest Physicians/La Société de Réanimation de Langue Française statement on competence in critical care ultrasonography. Chest. 2009; 135 (4): 1050 - 1060.

27 Lichtenstein D, Axler O. Intensive use of general ultrasound in the intensive care unit. Prospective study of 150 consecutive patients. Intensive Care Med. 1993; 19 (6): 353 - 355.

28 Havelock T, Teoh R, Laws D et al. Pleural procedures and thoracic ultrasound: British Thoracic Society Pleural Disease Guideline 2010. Thorax 2010; 65 (02): ii61–76

29 Piscaglia F, Nolsoe C, Dietrich CF et al. The EFSUMB Guidelines and Recommendations on the Clinical Practice of Contrast Enhanced Ultrasound (CEUS): update 2011 on non-hepatic applications. Ultraschall Med 2012; 33: 33–59

30 Michels G, Breitkreutz R, Pfister R. Value of lung ultrasound in emergency and intensive care medicine Dtsch Med Wochenschr. 2014 Nov;139(45):2301-7.

31 Gardelli G, Feletti F, Nanni A et al. Chest ultrasonography in the ICU. Respir Care 2012; 57: 773–781

32 Lichtenstein D, Goldstein I, Mourgeon E et al. Comparative diagnostic performances of auscultation, chest radiography, and lung ultrasonography in acute respiratory distress syndrome. Anesthesiology 2004; 100: 9–15

33 Lichtenstein DA. Lung ultrasound in the critically ill. Ann Intensive Care 2014; 4: 1

34 Lichtenstein DA Lung Ultrasound (in the Critically Ill) Superior to CT: The Example of Lung Sliding. Korean J Crit Care Med. 2017 Feb;32 (1):1-8.

35 Armbruster W, Eichholz R, Notheisen T. Lung Ultrasound for Anesthesia, Intensive Care and Emergency Medicine Anasthesiol Intensivmed Notfallmed Schmerzther. 2019 Feb;54 (2):108-127

36 Michels G, Breitkreutz R, Pfister R. Value of lung ultrasound in emergency and intensive care medicine Dtsch Med Wochenschr. 2014 Nov;139 (45):2301-7

37 Efremov SM, Kuzkov VV, Fot EV, Kirov MY, Ponomarev DN, Lakhin RE, Kokarev EA. J Lung Ultrasonography and Cardiac Surgery: A Narrative Review. Cardiothorac Vasc Anesth. 2020 Jan 23.

38 Ziskin, M. C, et al. The comet tail artifact." J Ultrasound Med. (1982)., 1, 1-7.

39 Dietrich CF, Mathis G, Blaivas M, Volpicelli G, Seibel A, Wastl D, Atkinson NS, Cui XW, Fan M, Yi D (2016) Lung B-line artefacts and their use. J Thorac Dis 8:1356–1365

40 Lesser TG. Significance of Thoracic and Lung Ultrasound in Thoracic Surgery. Ultraschall Med. 2017 Dec;38(6):592-610.

41 Goffi A, Kruisselbrink R, Volpicelli G. The sound of air: point-of care lung ultrasound in perioperative medicine. Can J Anesth 2018; 65: 399–416.

42 Clevert DA, D'Anastasi M, Jung EM. Contrast-enhanced ultrasound and microcirculation: efficiency through dynamics--current developments. Clin Hemorheol Microcirc. 2013;53(1-2):171-86.

43 Clevert DA, Jung EM. [Interventional sonography of the liver and kidneys]. Der Radiologe. 2013;53(11):962-73.

44 Chaloupka M, Bischoff R, Pfitzinger P, Lellig E, Ledderose S, Buchner A, Schlenker B, Stief C, Clevert DA, Apfelbeck M. Detection of Gleason 6 prostate cancer in patients with clinically significant prostate cancer on multiparametric magnetic resonance imaging. Clin Hemorheol Microcirc. 2019;73(1):105-111.

45 Apfelbeck M, Chaloupka M, Schlenker B, Stief CG, Clevert DA. Follow-up after focal therapy of the prostate with high intensity focused ultrasound (HIFU) using contrast enhanced ultrasound (CEUS) in combination with MRI image fusion. Clin Hemorheol Microcirc. 2019;73(1):135-143.

46 European Society of Radiology (ESR). Abdominal applications of ultrasound fusion imaging technique: liver, kidney, and pancreas. Insights Imaging. 2019 Jan 28;10(1):6.

47 Schlenker B, Apfelbeck M, Armbruster M, Chaloupka M, Stief CG, Clevert DA. Comparison of PIRADS 3 lesions with histopathological findings after MRI-fusion targeted biopsy of the prostate in a real world-setting. Clin Hemorheol Microcirc. 2019;71(2):165-170.

48 Rübenthaler J, Wilson S, Clevert DA. Multislice computed tomography/contrast-enhanced ultrasound image fusion as a tool for evaluating unclear renal cysts. Ultrasonography. 2019 Apr;38(2):181-187.

49 Schlenker B, Apfelbeck M, Buchner A, Stief C, Clevert DA. MRI-TRUS fusion biopsy of the prostate: Quality of image fusion in a clinical setting. Clin Hemorheol Microcirc. 2018;70(4):433-440.

50 Jung EM, Clevert DA. Contrast-enhanced ultrasound (CEUS) and image fusion for procedures of liver interventions. Radiologe. 2018 Jun;58(6):538-544

51 Apfelbeck M, Clevert DA, Ricke J, Stief C, Schlenker B. Contrast enhanced ultrasound (CEUS) with MRI image fusion for monitoring focal therapy of prostate cancer with high intensity focused ultrasound (HIFU). Clin Hemorheol Microcirc. 2018;69(1-2):93-100.

52 Müller-Peltzer K, Rübenthaler J, Reiser M, Clevert DA. Contrast-enhanced ultrasound (CEUS) of the liver: Critical evaluation of use in clinical routine diagnostics Radiologe. 2017 May;57(5):348-355.

53 Rübenthaler J, Paprottka KJ, Marcon J, Reiser M, Clevert DA. MRI and contrast enhanced ultrasound (CEUS) image fusion of renal lesions. Clin Hemorheol Microcirc. 2016;64(3):457-466.

54 Zimmermann H, Rübenthaler J, Paprottka P, Paprottka KJ, Reiser M, Clevert DA. Feasability of contrast-enhanced ultrasound with image fusion of CEUS and MS-CT for endovascular grafting in infrarenal abdominal aortic aneurysm in a single patient. Clin Hemorheol Microcirc. 2016;64(4):711-719.

55 Paprottka PM, Zengel P, Cyran CC, Paprottka KJ, Ingrisch M, Nikolaou K, Reiser MF, Clevert DA. Evaluation of multimodality imaging using image fusion with MRI and CEUS in an experimental animal model. Clin Hemorheol Microcirc. 2015;61(2):143-50.

56 Jung EM, Clevert DA. Possibilities of sonographic image fusion: Current developments Radiologe. 2015 Nov;55(11):937-48.

57 Paprottka PM, Zengel P, Cyran CC, Ingrisch M, Nikolaou K, Reiser MF, Clevert DA. Evaluation of multimodality imaging using image fusion with ultrasound tissue elasticity imaging in an experimental animal model. Clin Hemorheol Microcirc. 2014;57(2):101-10.

58 Clevert DA, Jung EM. Interventional sonography of the liver and kidneys Radiologe. 2013 Nov;53(11):962-73.

59 Clevert DA, D'Anastasi M, Jung EM. Contrast-enhanced ultrasound and microcirculation: efficiency through dynamics--current developments. Clin Hemorheol Microcirc. 2013;53 (1-2):171-86.

60 Clevert DA, Paprottka PM, Helck A, Reiser M, Trumm CG. Image fusion in the management of thermal tumor ablation of the liver. Clin Hemorheol Microcirc. 2012;52(2-4):205-16.

61 Helck A, Notohamiprodjo M, Danastasi M, Meinel F, Reiser M, Clevert DA. Ultrasound image fusion - clinical implementation and potential benefits for monitoring of renal transplants. Clin Hemorheol Microcirc. 2012;52(2-4):179-86.

62 Clevert DA, Helck A, Paprottka PM, Zengel P, Trumm C, Reiser MF. Ultrasound-guided image fusion with computed tomography and magnetic resonance imaging. Clinical utility for imaging and interventional diagnostics of hepatic lesions Radiologe. 2012 Jan;52(1):63-9.

63 Clevert DA, Helck A, D'Anastasi M, Gürtler V, Sommer WH, Meimarakis G, Weidenhagen R, Reiser M. Improving the follow up after EVAR by using ultrasound image fusion of CEUS and MS-CT. Clin Hemorheol Microcirc. 2011;49(1-4):91-104

64 Rennert J, Georgieva M, Schreyer AG, Jung W, Ross C, Stroszczynski C, et al. Image fusion of contrast enhanced ultrasound (CEUS) with computed tomography (CT) or magnetic resonance imaging (MRI) using volume navigation for detection, characterization and planning of therapeutic interventions of liver tumors. Clin Hemorheol Microcirc. 2011;49(1-4):67-81.

65 Soummer A1, Perbet S, Brisson H, Arbelot C, Constantin JM, Lu Q, Rouby JJ; Lung Ultrasound Study Group. Ultrasound assessment of lung aeration loss during a successful weaning trial predicts postextubation distress Crit Care Med. 2012 Jul;40(7):2064-72.

66 Lichtenstein DA, Meziere GA. Relevance of lung ultrasound in the diagnosis of acute respiratory failure: The BLUE protocol. Chest 2008; 134:117–25.

67 Lichtenstein DA. Ultrasound in the management of thoracic disease. Crit Care Med 2007; 35 (05): S250–261

68 Ball CG, Ranson K, Dente CJ, et al. Clinical predictors of occult pneumothoraces in severely injured blunt polytrauma patients: A prospective observational study. Injury 2009; 40:44–7.

69 Staub LJ, Biscaro RRM, Kaszubowski E, et al. Chest ultrasonography for the emergency diagnosis of traumatic pneumothorax and haemothorax: A systematic review and meta-analysis. Injury 2018; 49:457–66.

70 Alrajhi K, Woo MY, Vaillancourt C. Test characteristics of ultrasonography for the detection of pneumothorax. Chest 2012; 141:703–8.

71 Caiulo VA, Gargani L, Caiulo S, et al. Lung ultrasound characteristics of community-acquired pneumonia in hospitalized children. Pediatr Pulmonol 2013; 48:280-7.

72 Radzina M, Biederer J. Ultrasonography of the Lung.Rofo. 2019 Oct;191(10):909-923

73 Lichtenstein DA, Lascols N, Mezi ere G, et al. Ultrasound diagnosis of alveolar consolidation in the critically ill. Intensive Care Med 2004;30: 276–81.

74 Reissig A, Gorg C, Mathis G. Transthoracic sonography in the diagnosis of pulmonary diseases: a systematic approach. Ultraschall Med 2009; 30: 438–454

75 Reissig A, Copetti R, Mathis G et al. Lung ultrasound in the diagnosis and follow-up of community-acquired pneumonia: a prospective, multicenter, diagnostic accuracy study. Chest 2012; 142: 965–972

76 Blaivas M. Lung ultrasound in evaluation of pneumonia. J Ultrasound Med 2012; 31:823-6.

77 Badenes R, Lozano A, Belda FJ. Postoperative pulmonary dysfunction and mechanical ventilation in cardiac surgery. Crit Care Res Pract 2015; 2015:1–8.

78 Colins JD, Burwell D, Furmanski S et al. Minimal detectable pleural effusions. A roentgen pathology model. Radiology 1972; 105: 51–53

79 Gryminski J, Krakowka P, Lypacewicz G. The diagnosis of pleural effusion by ultrasonic and radiologic techniques. Chest 1976; 70: 33–37

80 Hassan M, Rizk R, Essam H, et al. Validation of equations for pleural effusion volume estimation by ultrasonography. J Ultrasound 2017; 20:267–71.

81 World Health Organization. Clinical management of severe acute respiratory infection when novel coronavirus (nCoV) infection is suspected, interim guidance [EB/OL]. [2020-01-13]. https://www.who.int/publications-detail/clinical-management-of-severe-acute-respiratory-infection-when -novel-coronavirus-(nCoV)-infection-is-suspected.

82 Chan JF, Yuan S, Kok KH, et al. A familial cluster of pneumonia associated with the 2019 novel coronavirus indicating person-to-person transmission: a study of a family cluster. Lancet 2020. DOI: 10.1016/S0140-6736(20)30154-9.

83 Wang W, Tang J, Wei F. Updated understanding of the outbreak of 2019 novel coronavirus (2019.nCoV) in Wuhan, China. J Med Virol 2020. Jan 29. doi:10.1002/jmv.25689. [Epub ahead of print].

84 Bai HX, Hsieh B, Xiong Z, Halsey K, Choi JW, Tran TML, Pan I, Shi LB, Wang DC, Mei J, Jiang XL, Zeng QH, Egglin TK, Hu PF, Agarwal S, Xie F, Li S, Healey T, Atalay MK, Liao WH. Performance of radiologists in differentiating COVID-19 from viral pneumonia on chest CT. Radiology. 2020 Mar 10:200823. doi: 10.1148/radiol.2020200823. [Epub ahead of print]

85 Peng QY1, Wang XT2, Zhang LN3; Chinese Critical Care Ultrasound Study Group (CCUSG). Findings of lung ultrasonography of novel corona virus pneumonia during the 2019-2020 epidemic. Intensive Care Med. 2020 Mar 12. doi: 10.1007/s00134-020-05996-6.

86 Yin W, Li Y, Zeng X, et al. The utilization of critical care ultrasound to assess hemodynamics and lung pathology on ICU admission and the potential for predicting outcome. PLoS One 2017; 12(8): e0182881.

87 Liu J, Feng X, et al. New guidelines for ultrasonic diagnosis of neonatal lung diseases. Chinese Journal of Contemporary Pediatrics 2019; 21(02):105-113.

88 Leech M, Bissett B, Kot M, et al. Lung ultrasound for critical care physiotherapists: a narrative review. Physiother Res Int 2015; 20(2): 69-76.

89 Yi Huang, Sihan Wang, Yue Liu, Yaohui Zhang, Chuyun Zheng, Yu Zheng, Chaoyang Zhang, Weili Min, Huihui Zhou, Ming Yu, Mingjun Hu A preliminary study on the ultrasonic manifestations of peripulmonary lesions of non-critical novel coronavirus pneumonia (COVID-19) https://ssrn.com/

At Siemens Healthineers, our purpose is to enable healthcare providers to increase value by empowering them on their journey towards expanding precision medicine, transforming care delivery, and improving patient experience, all enabled by digitalizing healthcare.

An estimated 5 million patients globally everyday benefit from our innovative technologies and services in the areas of diagnostic and therapeutic imaging, laboratory diagnostics and molecular medicine, as well as digital health and enterprise services.

We are a leading medical technology company with over 170 years of experience and 18,000 patents globally. With more than 48,000 dedicated colleagues in 75 countries, we will continue to innovate and shape the future of healthcare.

Standalone clinical images may have been cropped to better visualize pathology. The products/features mentioned in this document may not be commercially available in all countries. Due to regulatory reasons, their future availability cannot be guaranteed.

Please contact your local Siemens Healthineers organization for further details.

Siemens Healthineers Headquarters
Siemens Healthcare GmbH
Henkestr. 127
91052 Erlangen, Germany
Phone: +49 9131 84-0
siemens-healthineers.com

Legal Manufacturer
Siemens Medical Solutions USA, Inc.
Ultrasound
685 E. Middlefield Road
Mountain View, CA 94043, USA
Phone: 1-888-826-9702
siemens-healthineers.com/ultrasound

Published by Siemens Medical Solutions USA, Inc. · 9039 0420 online